



OPEN ACCESS

EDITED BY

Yi Chen,
Chinese Academy of Sciences (CAS), China

REVIEWED BY

Fulong Cai,
Chinese Academy of Sciences (CAS), China
Longyao Chen,
Chinese Academy of Geological Sciences
(CAGS), China

*CORRESPONDENCE

Xiaoying Liao,
✉ xyliao@nwu.edu.cn

RECEIVED 09 February 2025

ACCEPTED 07 April 2025

PUBLISHED 25 April 2025

CITATION

Wang G, Liao X, Liu L, Wang Y and Yang W
(2025) Reappraisal of the lithological units of
the Wuguan Complex: implication for the
Paleozoic evolution of the Qinling orogenic
belt.

Front. Earth Sci. 13:1573681.

doi: 10.3389/feart.2025.1573681

COPYRIGHT

© 2025 Wang, Liao, Liu, Wang and Yang. This
is an open-access article distributed under
the terms of the [Creative Commons
Attribution License \(CC BY\)](https://creativecommons.org/licenses/by/4.0/). The use,
distribution or reproduction in other forums is
permitted, provided the original author(s) and
the copyright owner(s) are credited and that
the original publication in this journal is cited,
in accordance with accepted academic
practice. No use, distribution or reproduction
is permitted which does not comply with
these terms.

Reappraisal of the lithological units of the Wuguan Complex: implication for the Paleozoic evolution of the Qinling orogenic belt

Ge Wang¹, Xiaoying Liao^{1*}, Liang Liu¹, Yawei Wang² and Wenqiang Yang¹

¹State Key Laboratory of Continental Evolution and Early Life, Department of Geology, Northwest University, Xi'an, China, ²Geological Party No.313 of Yunnan Nonferrous Metals Geological Bureau, Yuxi, China

The Wuguan Complex, located along the southern margin of the Shangdan suture zone, plays a critical role in investigating the tectonic evolution of the Qinling orogenic belt and constraining the collision timing between the North and South China Blocks. However, the age and provenance of lithological units within the Wuguan Complex, as well as its tectonic significance, remain subjects of ongoing debate. The U–Pb–Hf isotopic analysis of detrital zircons from the meta-sedimentary rocks of the Wuguan Complex reveals distinctly different age patterns and depositional ages, which can be subdivided into a Devonian (ca. 380–400 Ma) unit and a Mid-Neoproterozoic (732–743 Ma) unit. The Devonian unit has a detrital age spectrum with two main peaks at ~440 and ~893 Ma, interpreted to reflect a mixed source derived from the early Paleozoic North Qinling magmatic arc and the Neoproterozoic South Qinling basement, corresponding to the Devonian Liuling Group in the South Qinling. The Mid-Neoproterozoic unit has an age spectrum with a dominant peak at ~898 Ma, interpreted to be primarily derived from widespread Neoproterozoic South Qinling volcanic and plutonic rocks. The meta-mafic volcanic rocks in the Wuguan Complex have a mean weighted zircon U–Pb age of 436 ± 6 Ma, exhibit high TiO₂ contents with both E-MORB and OIB affinities, and show depleted zircon $\epsilon_{\text{Hf}}(t)$ values, indicating formation within an intraplate tectonic setting. Combining these findings with previous data, we propose a reappraisal of the lithological units in the Wuguan Complex, which includes (1) the Mid-Neoproterozoic (ca. 732–743 Ma) sedimentary unit developed on the ancient South Qinling basement (2) the Silurian (ca. 430–440 Ma), meta-mafic volcanic unit, indicative of a local tectonic transition in the South Qinling belt from compressional to extensional during the Silurian, and (3) the Devonian (ca. 380–400 Ma) sedimentary unit, correlative with the Devonian Liuling Group, which was deposited during the final stages of closure of the Paleo-Qinling Ocean. These units were structurally juxtaposed by ductile strike-slip faults during the Early Carboniferous.

KEYWORDS

Wuguan Complex, lithological units, zircon U-Pb-Hf isotopes, geochemistry, qinling orogenic belt

1 Introduction

The Qinling orogenic belt, located between the North China Block and the South China Block, plays a crucial role in understanding the tectonic evolution of the East Asian continental crust. It is widely regarded as a collage of multiple orogenic systems, recording geological evolution from at least the Neoproterozoic to the Mesozoic (Zhang G. W. et al., 1995; 2001; Meng and Zhang, 2000; Ratschbacher et al., 2003; Wu and Zheng, 2013; Liu et al., 2016; Dong and Santosh, 2016; Dong et al., 2021; Xu et al., 2020; Bader et al., 2013; 2025). The North Qinling Belt is generally considered to record Early Paleozoic tectonic evolution, including oceanic crust subduction (Meng and Zhang, 2000; Dong et al., 2011a; Dong and Santosh, 2016), deep continental subduction/HP-UHP metamorphism (Yang et al., 2003; Liu et al., 2013; Wu and Zheng, 2013; Wang et al., 2014; Liao et al., 2016; Gong et al., 2016; Chen et al., 2021), and subsequent uplift events and accompanied by magmatism (Zhang et al., 2013; Liu et al., 2016; Dong et al., 2018). However, the timing of the closure of the Paleo-Qinling ocean remains a critical issue. Some scholars contend that the Ocean closed as late as the Silurian or even Early Ordovician, along the Shangdan suture zone, which is generally considered as the main boundary between the North China block and the Yangtze block (Mattauer et al., 1985; Gao et al., 1995; Zhang et al., 2001; Liu et al., 2016; Ren et al., 2019; Dong et al., 2011b; Dong et al., 2013; Dong et al., 2021). Others propose the existence of the Paleo-Qinling Ocean existed from the Early Paleozoic to Triassic, ultimately closed during the Indosinian orogeny, which resulted in the welding of the North China and South China blocks (Yan et al., 2012; 2016; Chen et al., 2014a,b, 2020; Meng, 2017; Li et al., 2020; Bader et al., 2025).

The Wuguan Complex, a key tectonic unit along the southern margin of the Shangdan suture zone, has been a focal point in studies of the Qinling orogen's evolution (Yu et al., 1988; Zhang et al., 1988; Pei et al., 1997; Dong et al., 2013; Chen et al., 2014a; 2020; Yan et al., 2016; Jiang et al., 2017; Li et al., 2020; Bader et al., 2025). The Wuguan Complex is generally described as a tectonic mélange containing highly variable lithological assemblages that have undergone amphibolite-facies metamorphism (Pei et al., 1996; Yan et al., 2016; Li et al., 2020). Its age, provenance, and tectonic significance remain subjects of ongoing debate. Previous studies have proposed various tectonic scenarios for the Wuguan Complex, including (1) an Early Paleozoic post-orogenic molasse related to the collision of the NCB and SCB (Mattauer et al., 1985), (2) a fore-arc accretionary prism associated with subduction of the Paleo-Qinling Ocean during the Early or Late Paleozoic (Meng, 1994; Yu and Meng, 1995; Zhang et al., 2001; Dong et al., 2013), (3) formation in a rift environment during the Neoproterozoic (Pei et al., 1997; Lu et al., 2003; Shi et al., 2013), and (4) formation in a long-lived fore-arc basin on the southern margin of the North Qinling belt during the Devonian to Early Carboniferous (Yan et al., 2016; Li et al., 2020), which corresponds to a westward continuation of the Guishan Complex of the Dabie orogen (Chen et al., 2014a; 2020; 2021). Clearly, accurately determining the composition and formation age of the Wuguan Complex is critical for constraining the tectonic evolution of the Qinling orogenic belt.

In this study, we present new petrological observations, zircon U–Pb geochronology, and Lu–Hf isotope data for meta-sedimentary and meta-volcanic rocks, along with geochemical analyses of meta-mafic volcanic rocks from the Wuguan Complex

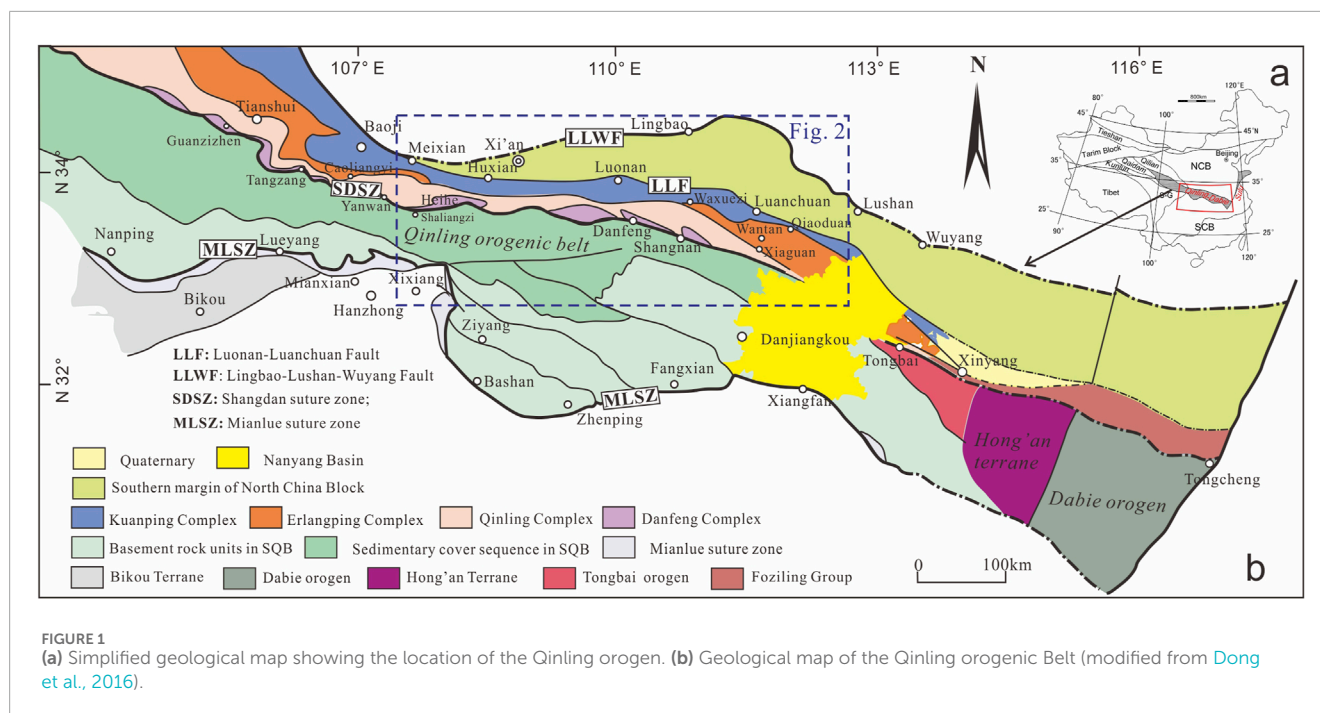
in the Danfeng–Shangnan area. The new provenance data, combined with regional geological and geochronological information, enable us to reevaluate the depositional ages, provenance, stratigraphic correlations, and tectonic setting of the Wuguan Complex. Furthermore, these findings help clarify the relationship of the Wuguan Complex to the broader Paleozoic tectonic evolution of the Qinling orogen.

2 Geological setting

The Qinling orogenic belt (QOB) located between the NCB and SCB (Figure 1a) is divided into the North Qinling belt (NQB) and South Qinling belt (SQB) by the Shangdan suture (Zhang G. W. et al., 1995; 2001; Meng and Zhang, 2000; Dong et al., 2011a) (Figure 1b).

The NQB consists of Kuanping Complex, Erlangping Complex, Qinling Complex and Danfeng Complex mélange separated from each other by thrust faults or ductile shear zones (Figure 2a). The Kuanping Complex is located in the northernmost part of NQB, which is mainly composed of clastic rocks, meta-volcanics and marbles (Zhang et al., 1991; Liu et al., 1993). The Erlangping Complex is composed of lower amphibolite-facies mafic volcanics, clastic sedimentary successions, and carbonates (Zhang et al., 2001). The Qinling Complex, as a major part of the NQB, consists of gneisses, schists, amphibolites, marble-calc-silicate rocks and HP-UHP rocks. The HP-UHP metamorphic rocks were believed to the products of deep continental subduction and experienced UHP metamorphism at ca. 500–490 Ma (Yang et al., 2003; Liu et al., 2013; 2016; Wang et al., 2011; Chen et al., 2015; Liao et al., 2016; Gong et al., 2016; Liu et al., 2016). Additionally, Early Neoproterozoic gneissic granites and widespread Early Paleozoic granites are also represented in Qinling Complex (Lu et al., 2003; Chen et al., 2006; Zhang et al., 2013; Wang et al., 2003; 2013c and reference therein). The Shangdan suture zone, separated the North Qinling belt from the South Qinling, was traditionally considered as the most important boundary between the North China and the South China Block, (Mattauer et al., 1985; Zhang Q. et al., 1995; Zhang et al., 2001; Dong et al., 2011c; Dong et al., 2013; Dong et al., 2017). The suture zone exposes ophiolitic assemblages, and subduction-related volcanic and sediments (Zhang et al., 1995b; Yu et al., 1988; Dong, et al., 2011b; 2013). An Ordovician to Silurian radiolarians has been found in bedded cherts and constrain the time of formation (Cui et al., 1995). The formation age of the ophiolitic suite has been well constrained as 534 ± 9 Ma to 517.8 ± 2.8 Ma (Dong et al., 2011b; Li et al., 2015; Liu et al., 2016). The formation age of the island-arc rocks has been constrained as 507 ± 3 to 499.8 ± 4.0 Ma (Pei et al., 2005; Lu et al., 2009), indicating continued subduction of the Shangdan oceanic lithosphere at ca. 500 Ma (Liu et al., 2016).

The SQB is located between the Shangdan suture zone in the north and the Mianlue suture zone in the south (Figure 1a), and consists of basement and sedimentary cover. The basement rocks mainly include the Douling and Xiaomoling Complexes, and the Wudangshan and Yaolinghe Groups (Zhang et al., 1988; Zhang et al., 2001). Excluding the protolith of the granitic gneiss from the Douling Complex yielded ages of ca. 2.51–2.47 Ga (Hu et al., 2013; Nie et al., 2016), other basement rocks are mainly characterized by early-middle Neoproterozoic (680–860 Ma) volcanic rocks (Lu et al., 2009; Niu et al., 2006; Liu et al., 2011; Ling et al., 2007; Xia et al., 2008; Ling et al., 2010; Li Z. X. et al., 2003).



Along the northern margin of the SQB, the Wuguan Complex (to the north) and the Middle to Upper Devonian Liuling Group (to the south) are exposed adjacent to each other (Figure 2a). The Wuguan Complex is bounded by the Shangdan suture zone to the north and the Mianyuzui–Maanqiao ductile shear zone to the south (Yu et al., 1988; Yu and Meng, 1995; Dong et al., 2013). It is generally regarded as a dismembered sedimentary prism (or accretionary wedge) that likely represents an independent, metamorphosed equivalent of the Devonian Liuling Group (Pei et al., 1996). The lithologies of the Wuguan Complex are highly variable, and all rocks have undergone intense deformation and amphibolite-facies metamorphism (Yan et al., 2016; Li et al., 2020; Chen et al., 2021; Sheir et al., 2024; Bader et al., 2025), transforming most of the rocks into gneisses, schists, or mylonites. Based on differences in lithological assemblages, Pei et al. (1996) subdivided the Wuguan Complex into six distinct rock units separated by ductile shear zones (Figures 2b, c): (1) Shimazhai unit dominated by garnet-bearing marble and carbonaceous schist, with interlayers of garnet-bearing two-mica quartz schist and mica quartzite; (2) the Diaozhuang Unit, consisting of staurolite-bearing mica quartz schist and epidote-bearing mica quartz schist (Figure 3a), with pyrite- or scapolite-bearing marble and siliceous marble; (3) the Balipo Unit, characterized by light-grey, fine-grained diopside-bearing marble, with minor quartzite and biotite quartz schist; (4) the Maoping Unit, comprising garnet-bearing metapsammite (Figures 3b, c), with minor marble and lenticular amphibolite, and mylonites recognized in the eastern part of the unit; (5) the Mianyuzui unit, predominantly green meta-mafic volcanic rocks (Figure 3d), with minor interlayers of garnet-bearing biotite schist, garnet-bearing mica quartz schist, and thin marble (Figures 3e, f); folded meta-mafic volcanic bands within the marble suggest a sinistral ductile strike-slip shearing (Figure 3f), which is also supported by various kinematic features such as σ and δ -type porphyroblasts, mica-fishes, and amphibole-fishes in the mylonites (Chen et al., 2021; Sheir et al.,

2024); and (6) the Hualing Unit, mainly augen felsic mylonite, formed by deformation of felsic veins and marking the tectonic boundary between the Wuguan Complex and the Liuling Group. Geometric and kinematic evidence indicates that the Mianyuzui ductile shear zone underwent two phases of deformation: the early thrust from north to south and the late sinistral strike-slip during the Late Permian (Chen et al., 2021; Sheir et al., 2024).

South of the Wuguan Complex, the Middle to Upper Devonian Liuling Group is exposed between the Mianyuzui–Maanqiao and Shanyang–Fengzhen faults (Figure 2a). It is characterized by thick-bedded, low-grade metamorphosed (greenschist-facies) gray-green sandstone, siltstone, slate, and minor conglomerate (Hacker et al., 2004; He et al., 2005; Yan et al., 2007; Dong et al., 2013; Liao et al., 2017). Recent studies integrating detrital zircon U–Pb ages and Hf isotopes demonstrate that Liuling sediments were sourced from both the North and South Qinling belts (Dong et al., 2013; Liao et al., 2017; Ren et al., 2019), and formed in a foreland basin or passive margin setting after the main collision (Gao et al., 1995; Zhang et al., 2001; Dong et al., 2013; Ren et al., 2019).

3 Sample descriptions

In this study, we collected representative samples from the main lithological units of the Wuguan Complex in the Danfeng–Shangnan area (Figure 2b). We focused on meta-sedimentary rocks (psammitic and pelitic schists) and meta-volcanic rocks (amphibolites) for petrography and zircon U–Pb–Hf analysis.

Sample 15WG-08 from Maoping unit is a garnet bearing meta-psammite, comprising subangular to subrounded plagioclase (40%–50%), quartz (15%–20%), biotite (10%–15%), garnet (<5%), minor amphibole (<5%) fragments, and a clay matrix (Figure 4a), probably indicating a protolith of arkose. Garnet and amphibole

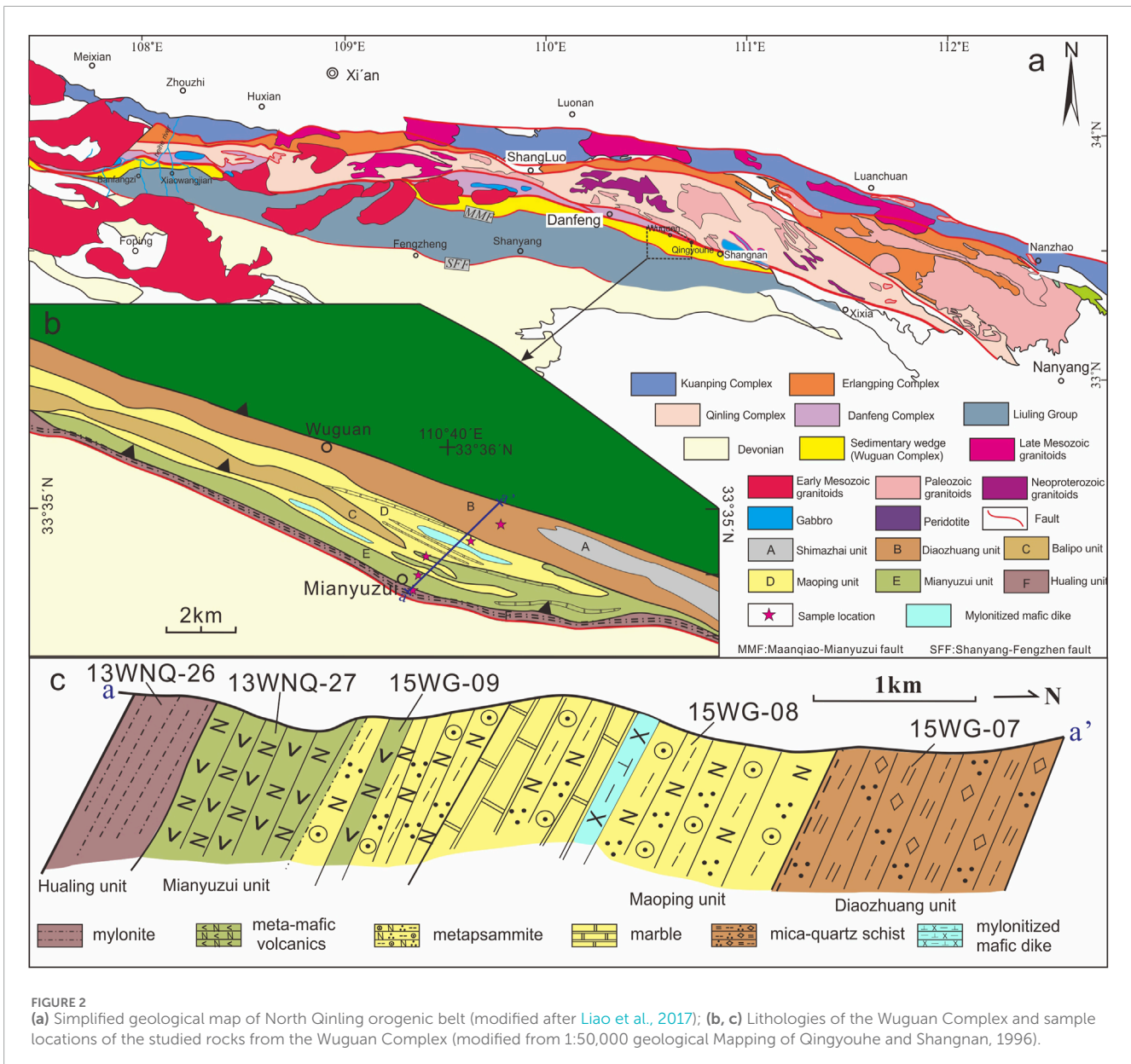


FIGURE 2 (a) Simplified geological map of North Qinling orogenic belt (modified after Liao et al., 2017); (b, c) Lithologies of the Wuguan Complex and sample locations of the studied rocks from the Wuguan Complex (modified from 1:50,000 geological Mapping of Qingyouhe and Shangnan, 1996).

occur sporadically throughout the sample, and nearly all quartz grains show signs of recrystallization (Figure 4b).

Sample 15WG-07 from Diaozhuang unit is a high deformed mica-quartz schist. It consists of quartz (40%–50%), plagioclase (10%–25%), muscovite (10%–20%), biotite (20%–25%), and garnet (<5%) (Figure 4c). Quartz grains exhibit partial recrystallization and are distinctly preferred. Biotite distributes along the cleavage with preferred orientation. Garnet porphyroblast is commonly idiomorphic with some quartz inclusions in the core and shows helicitic structure.

Sample 13WNQ-26 from Hualing unit is a meta-psammite, mainly composed of quartz (~55%) and plagioclase (~35%) and abundant biotite fragments (15%–20%) (Figure 4c). The quartz grains exhibit undulatory extinction.

Two amphibolite samples 13WNQ-27 and 15WG-09 are selected from Mianyuzui and layer (~50 m) of Maoping units,

are primarily composed of amphibole, plagioclase, biotite, and epidote (Figures 4e, f). Amphibole is strongly oriented to form the foliation of the rock.

All samples are shown in Table 1 and analytical methods are presented in Supplementary Appendix A1.

4 Result

4.1 Zircon U-Pb ages

Zircons from four samples, including three metasedimentary samples (15WG-07, 15WG-08, and 13WNQ-26) and one amphibolite sample (13WNQ-27), were dated. Detailed results for the zircon U-Pb dating are presented in Supplementary Table S1, and the zircon trace element data are

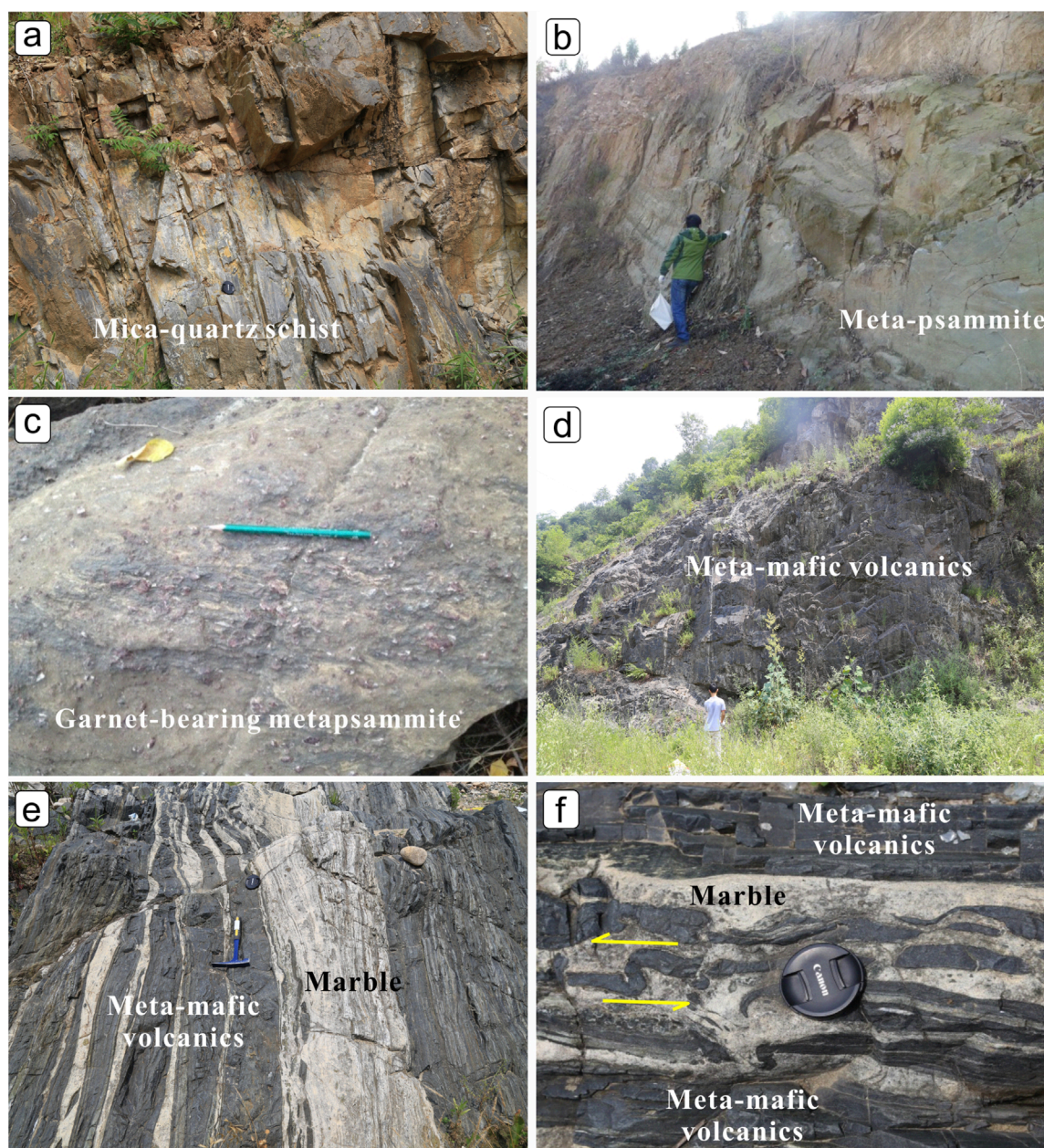


FIGURE 3
Field photographs of all studied samples from Wuguan Complex. (a) Mica-quartz schist from Diaozhuang unit; (b) Metapsammite from Hualing unit; (c) Garnet-bearing metapsammite from Maoping unit; (d) Meta-mafic volcanics from Mianyuzui Unit; (e) Green Meta-mafic volcanics with thinner marble layers; (f) The folded Meta-mafic volcanics bands in the marble.

provided in [Supplementary Table S2](#). Ages older than 1,000 Ma were calculated using the $^{207}\text{Pb}/^{206}\text{Pb}$ ratios, while younger ages were determined from the $^{206}\text{U}/^{208}\text{Pb}$ ratios. Most zircon U–Pb analyses are concordant or near concordant, with age concordance ranging from 90% to 110%.

4.1.1 Detrital zircon ages from meta-sedimentary rocks

In sample 15WG-07 (mica–quartz schist, Devonian unit), zircons are rounded to subhedral and range in size from

50 to 120 μm . CL imaging shows that all analyzed grains exhibit oscillatory or banded zoning ([Figure 5a](#)). Most zircon grains have high Th/U ratios (0.13–1.37) ([Figure 7e](#); [Supplementary Table S1](#)) and display similar chondrite-normalized REE patterns, which are strongly enriched in HREE and depleted in LREE ($\text{Gd}_N/\text{Yb}_N = 0.01\text{--}0.17$), with pronounced negative Eu anomalies ($\text{Eu}/\text{Eu}^* = 0.02\text{--}0.65$) ([Figure 7a](#); [Supplementary Table S2](#)). A total of ninety analyses were performed, of which 78 were concordant. These concordant grains yielded apparent ages ranging from 407 Ma to 2,653 Ma ([Figure 6a](#)). The grains fall into three primary age groups:

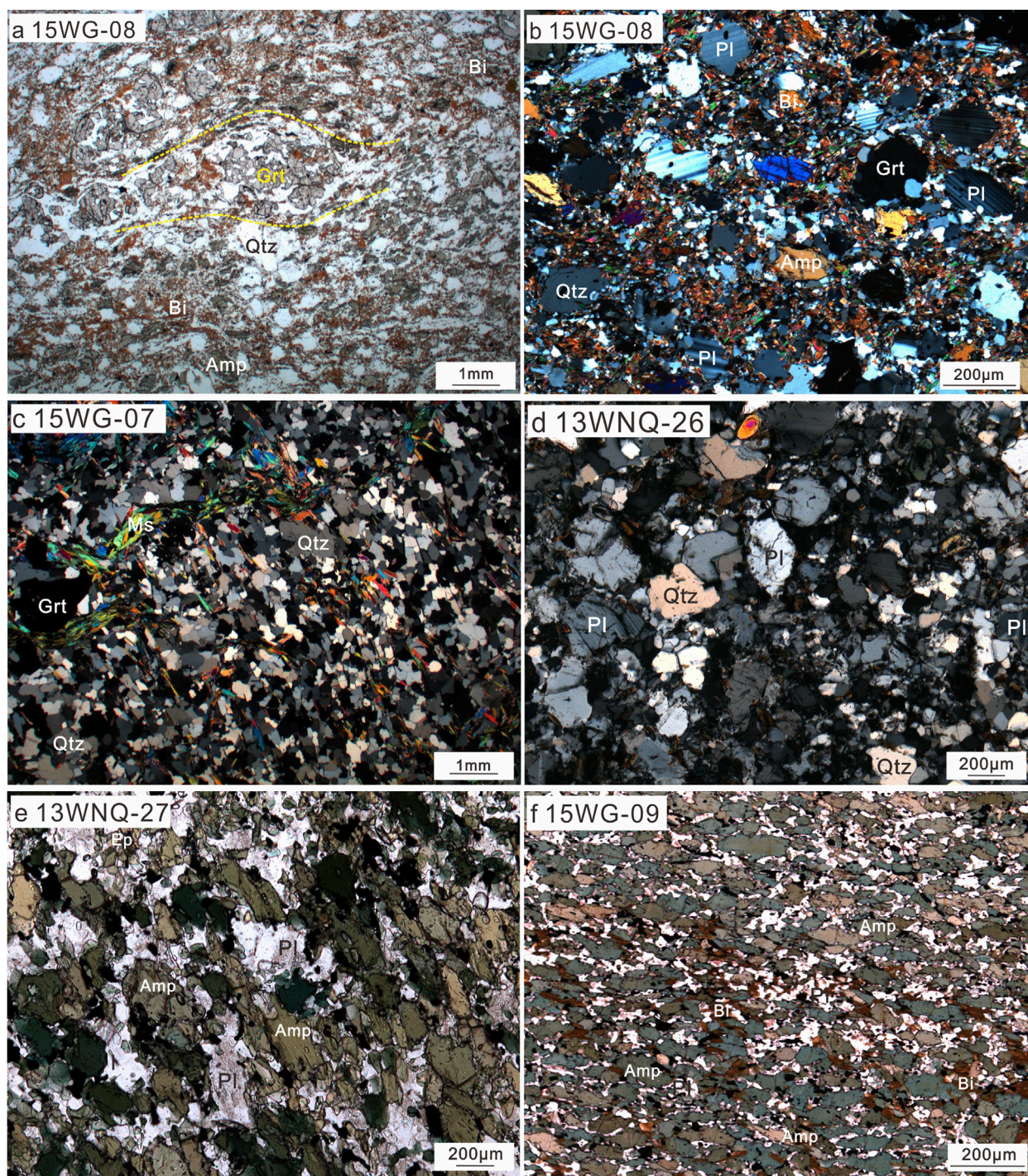


FIGURE 4

Photomicrographs illustrating the mineral assemblages of studied rocks in the Wuguan Complex. **(a)** Garnet bearing metapsammite 15WG-08 comprising subangular to subrounded plagioclase, quartz, biotite, minor garnet and amphibole fragments; **(b)** Garnet and amphibole occur sporadically throughout the sample 15WG-08; **(c)** Mica-quartz schist 15WG-07 consists of quartz, plagioclase, muscovite, biotite, and garnet; **(d)** Metapsammite 13WNQ-26 composed of quartz and plagioclase and abundant biotite fragments; **(e, f)** Meta-mafic volcanics 13WNQ-27 and 15WG-09 are primarily composed of amphibole, plagioclase, biotite, and epidote. Amp-amphibole, Pl-plagioclase, Grt-garnet, Qtz-quartz, Ms-Muscovite, Bi-biotite, Ep-Epidote.

407–505 Ma ($n = 36$), 632–896 Ma ($n = 22$), and 1,191–1825 Ma ($n = 19$). Only two grains yielded older ages of $2,459 \pm 15$ Ma and $2,653 \pm 11$ Ma. In the age spectrum, a prominent peak is

observed at 444 Ma, with subsidiary peaks at 760 Ma, 895 Ma, and 1,461 Ma. The youngest three concordant grains have $^{206}\text{Pb}/^{238}\text{U}$ ages of 407 ± 3 Ma, 413 ± 5 Ma, and 413 ± 3 Ma, with a weighted

TABLE 1 Sample localities, mineral assemblages and zircon U-Pb ages of the studied samples from the Wuguan Complex.

Sample	Location	Coordinates	Lithology	Mineral assemblage	Youngest detrital Zircon age or crystallization Age/Ma	Peak Ages/Ma
15WG-07	Diaozhuang	N 33°34' 43.1" E 110°40' 25.6"	mica-quartz schist	Qtz (40–50%) + Pl (10–25%) + Mu (10–20%) + Bi(20–25%) + Grt (<5%)	407 ± 3	440, 763, 892, 1,168, 1,386, 2,419
15WG-08	Maoping	N 33°34' 45.8" E 110°39' 24.3"	metapsammite	Pl (40–50%) + Qtz (10–20%) + Grt (<5%) + Amp (<5%)	741 ± 4	791, 839, 1,543, 1,685, 1824, 2,495
13WNQ-26	Hualing	N 33°33' 41.9" E 110°39' 20.1"	metapsammite	Qtz (~55%) + Pl (~35%) + Bi (15–20%)	310 ± 3	353, 756, 832, 906, 938
13WNQ-27	Mianyuzui	N 33°33' 49.2" E 110°39' 24.3"	metabasalt	Amp + Pl + Bi	436 ± 6	
15WG-09		N 33°34' 08.5" E 110°39' 32.8"				

mean age of 410 ± 9 Ma (MSWD = 1.3) (Supplementary Table S2), which we interpret as the maximum depositional age of this sample.

In sample 15WG-08 (garnet-bearing meta-psammite, Maoping Unit), zircons are rounded to subhedral and range in size from 50 to 200 μm , displaying oscillatory or banded zoning (Figure 5b). Most zircons exhibit similar steep HREE patterns ($Gd_N/Yb_N = 0.01\text{--}0.11$) and pronounced negative Eu anomalies ($Eu/Eu^* = 0.02\text{--}0.83$) (Figure 7b; Supplementary Table S2). Of the eighty-eight analyzed zircons, 76 usable analyses with high Th/U ratios (0.08–1.68) (Figure 7e; Supplementary Table S1) yielded ages ranging from 741 Ma to 2,561 Ma. The age spectrum shows a dominant population ranging from 741 Ma to 890 Ma ($n = 48$), which accounted for 61% of all zircons, with prominent peaks at ~791 Ma and ~839 Ma. Additionally, the age spectrum reveals two subdominant populations at 1,021–1791 Ma and 1972–2,561 Ma, with corresponding peaks at ~1,543 Ma, ~1,685 Ma, ~1824 Ma, and ~2,495 Ma (Figure 6b). The youngest concordant zircons range from ca. 741 to 759 Ma, giving a weighted mean of 748 ± 5 Ma.

Zircons from sample 13WNQ-26 (meta-psammite, Hualing Unit) are rounded to elongate and range in size from 50 to 150 μm , displaying oscillatory zoning or nebulous zoning with thin overgrowths (Figure 5c). Most zircons exhibit strongly negative Eu anomalies ($Eu/Eu^* = 0.01\text{--}0.51$) (Figure 7c; Supplementary Table S2) and high Th/U ratios (>0.4) (Figure 7e; Supplementary Table S1), characteristic of magmatic zircon. The overgrowth rims, however, show a less HREE-enriched pattern, with no Eu anomalies and low Th/U ratios (0.004–0.17) (Figure 7e). A total of sixty U-Pb analyses were performed, with 12 discarded due to high discordance. The remaining 48 concordant analyses yielded ages ranging from 309 Ma to 2,302 Ma (Figure 6c). The dominant age cluster is Neoproterozoic (730–931 Ma) with a main peak at

~869 Ma (80% of grains), and subordinate peaks at ~834 Ma and ~928 Ma. The oldest grains are 1,543 Ma and 2,302 Ma. A distinct group of seven analyses from zircon rims ranges 309–363 Ma with a weighted mean of 351 ± 11 Ma (MSWD = 6.1) and very low Th/U (<0.1), consistent with metamorphic zircon growth during a later event (see details in Discussion). Excluding these metamorphic ages, the youngest detrital zircon population in 13WNQ-26 ranges 732–763 Ma (mean 746 ± 7 Ma), similar to sample 15WG-08 which shows youngest detrital ages of 741–759 Ma (mean 748 ± 5 Ma).

4.1.2 Zircon ages from amphibolites

Zircons from amphibolite sample 13WNQ-27, ranging in size from 50 to 200 μm , are short prismatic grains. In CL images, most zircons display weak oscillatory or patchy zoning with low luminescence (Figure 5d). These zircons exhibit similar steep HREE patterns with negative Eu anomalies ($Eu/Eu^* = 0.001\text{--}1.70$) (Figure 7d; Supplementary Table S2), and most have Th/U ratios >0.3 (Figure 7e; Supplementary Table S1), characteristic of magmatic zircons.

A total of ninety U-Pb analyses were conducted on zircons from this sample, with 80 concordant analyses yielding apparent ages ranging from 418 Ma to 2,771 Ma (Figure 6d). Notably, 15 analyses define a cluster of Late Silurian–Early Devonian ages (418–482 Ma) with a weighted mean of 436 ± 6 Ma (Th/U = 0.21–2.25). We interpret this ~440 Ma population as representing igneous crystallization ages. Based on the largest coherent subset of these data, a mean weighted age of 436 ± 6 Ma is obtained, which we consider that the best estimate of the crystallization age of the amphibolite protolith. However, importantly, we also detected a number of older ages range from ~800 Ma to ~2,500 Ma. These older ages clearly indicate the presence of inherited (detrital or xenocrystic) zircons in the amphibolite. In fact, the age spectrum of 13WNQ-27 looks qualitatively similar to those of

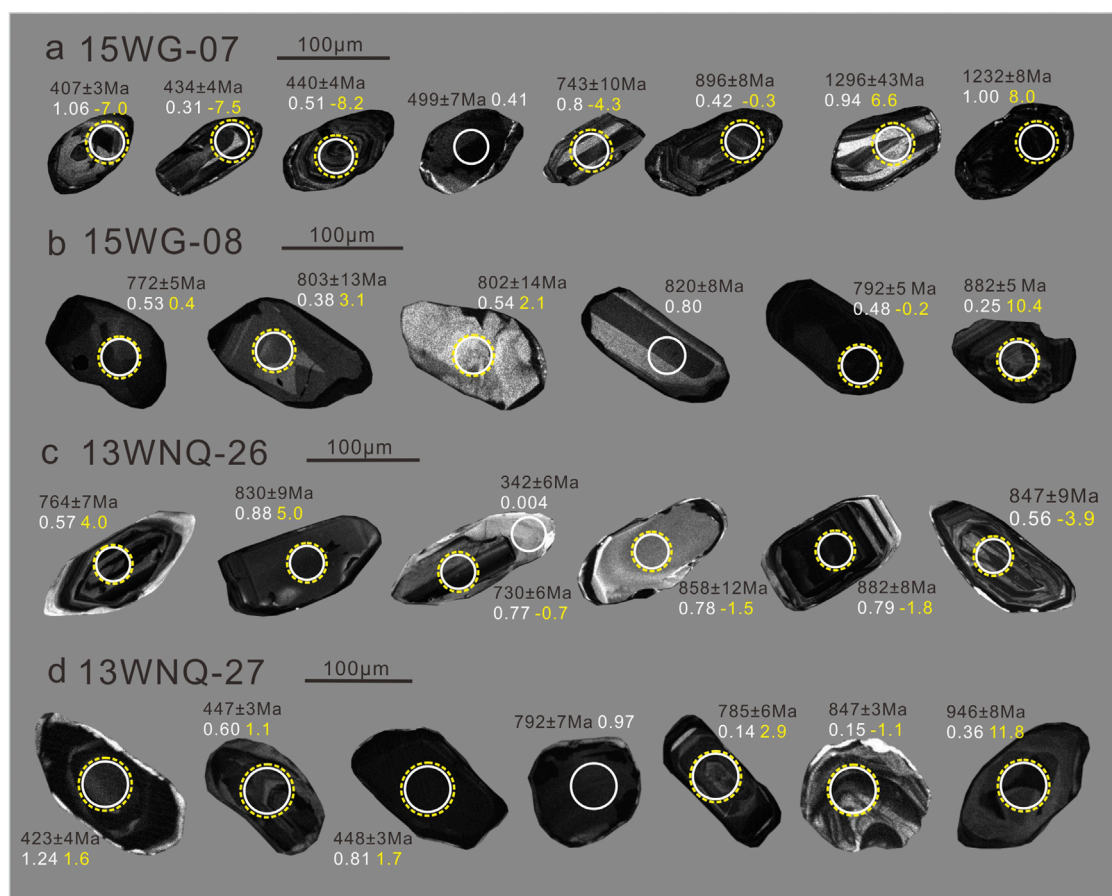


FIGURE 5

Representative CL images of zircon grains from Wuguan Complex. White circles with 32 μm diameter and yellow circles with 44 μm diameter represent U-Pb dating and Lu-Hf isotopic analysis points, respectively.

the metasedimentary samples (containing late Neoproterozoic and Paleozoic peaks) which suggests that the magma that formed this amphibolite assimilated crustal material or that the rock has a volcanoclastic component.

4.2 Zircon Hf isotopic composition

For Hf isotope analysis, zircons representing the major groups within their age populations were selected. The zircon Hf isotopic results are presented in Zircon Hf isotopic results are present in Figure 8 and Supplementary Table S3.

In sample 15WG-07, fifty-seven analyses from yield the $\epsilon_{\text{Hf}}(t)$ values varied from -14.3 to $+12.6$, with most of the grains showing Proterozoic model ages. The Early Palaeozoic zircons can be divided into two groups based on their $\epsilon_{\text{Hf}}(t)$ values. Group I zircons have positive $\epsilon_{\text{Hf}}(t)$ values ranging from $+0.3$ to $+12.6$, with a peak at $+7.45$, while Group II zircons have negative $\epsilon_{\text{Hf}}(t)$ of -0.2 to -14.3 , with a peak of -6.57 . Almost of the Meoproterozoic zircons have positive $\epsilon_{\text{Hf}}(t)$ values ranging from $+0.6$ to $+11.4$ (Figure 8a; Supplementary Table S3).

Sample 15WG-08 show $\epsilon_{\text{Hf}}(t)$ values range from -14.8 to $+11.5$, with forty eight ($\sim 70\%$ of total) positive $\epsilon_{\text{Hf}}(t)$ values

(Figure 8a; Supplementary Table S3), indicating a contribution of juvenile material to the sedimentary provenance.

Sample 13WNQ-26 yield the $\epsilon_{\text{Hf}}(t)$ values varied from -12.5 to $+6.0$, with most of the grains showing Meo- or Neo-Proterozoic model ages (Figure 8a; Supplementary Table S3).

In amphibolites sample 13WNQ-27, twenty nine analyses from show high $^{176}\text{Lu}/^{177}\text{Hf}$ ratios of 0.000391 – 0.002337 , and their $^{176}\text{Hf}/^{177}\text{Hf}$ ratios vary from 0.281694 to 0.282914 . The dominant zircons, with mean ages of 436 ± 6 Ma, have $\epsilon_{\text{Hf}}(t)$ values ranging from -4.4 to 13.7 (peak at -0.5) (Figure 8b; Supplementary Table S3) and Hf model ages ranging from 551 to $1,698$ Ma. Xenocrystic zircons, with U-Pb ages in the 746 – 968 Ma population, mainly exhibit variable $\epsilon_{\text{Hf}}(t)$ values from -2.2 to 16.4 , and the calculated Hf model ages ($T_{\text{DM}2}$) ranging from 729 to 1931 Ma.

4.3 Whole-rock major and trace elements for the meta-mafic rocks

The whole-rock element compositions of the massive and intercalated amphibolite samples from Wuguan Complex are listed in Supplementary Table S4. All amphibolite samples are tholeiitic basaltic rocks. They have low contents of SiO_2 (45.47 – 48.29 wt%),

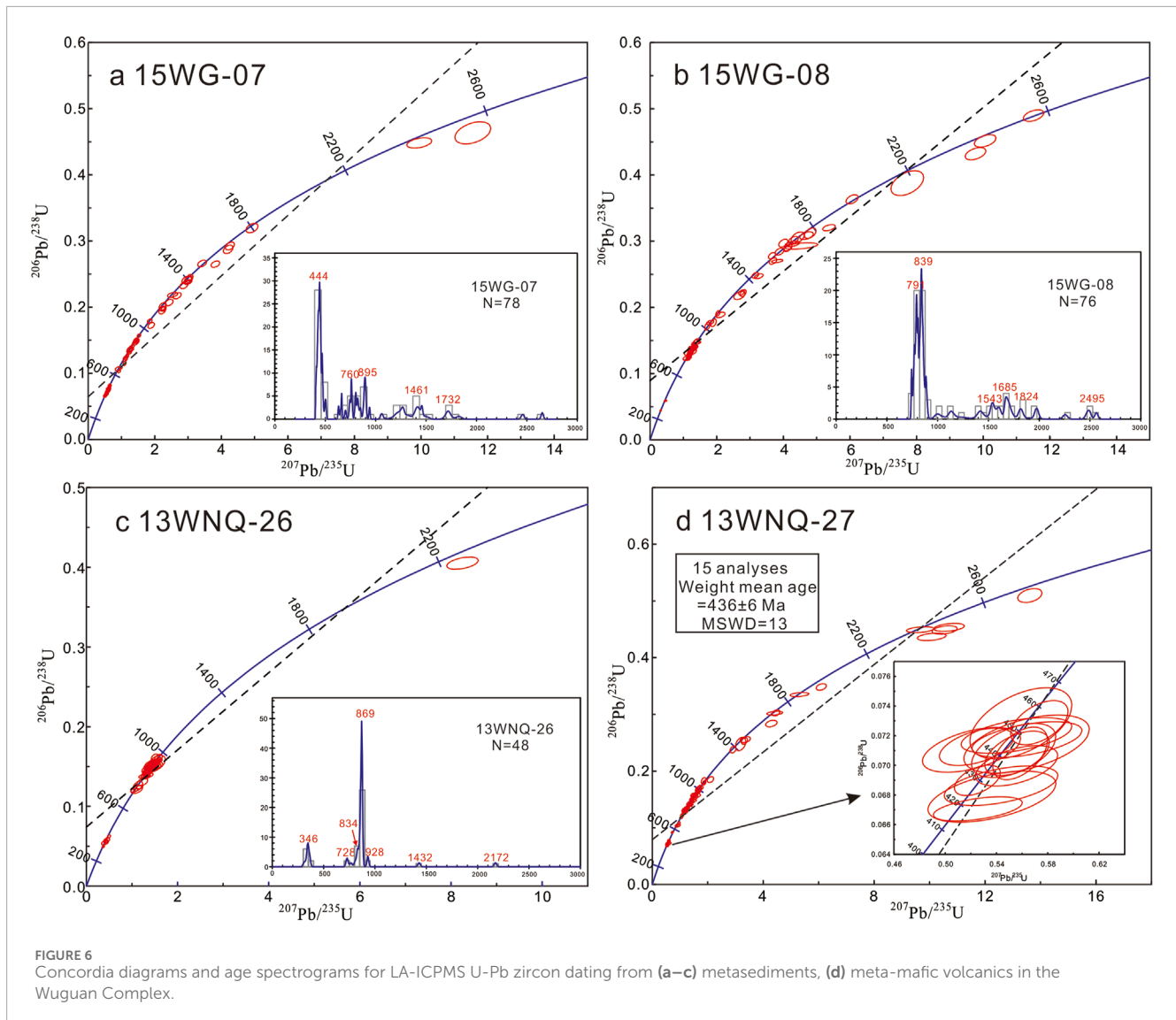


FIGURE 6 Concordia diagrams and age spectrometry for LA-ICPMS U-Pb zircon dating from (a–c) metasediments, (d) meta-mafic volcanics in the Wuguan Complex.

Na_2O (2.56–4.18wt%), K_2O (0.43–1.08wt%) contents, with very low $\text{K}_2\text{O}/\text{Na}_2\text{O}$ ratios of 0.12–0.5, but high contents of $\text{Fe}_2\text{O}_3^{\text{T}}$ (12.89–14.41 wt%), $\text{Mg}^{\#}$ values (39–56), and TiO_2 (1.74–3.03wt%). All amphibolite samples fall within the alkaline basalt fields on the $\text{Na}_2\text{O} + \text{K}_2\text{O}$ vs. SiO_2 diagram (Figure 9a) of Middlemost (1994). They have sub-alkaline affinities and follow a tholeiitic differentiation trend (Figure 9b).

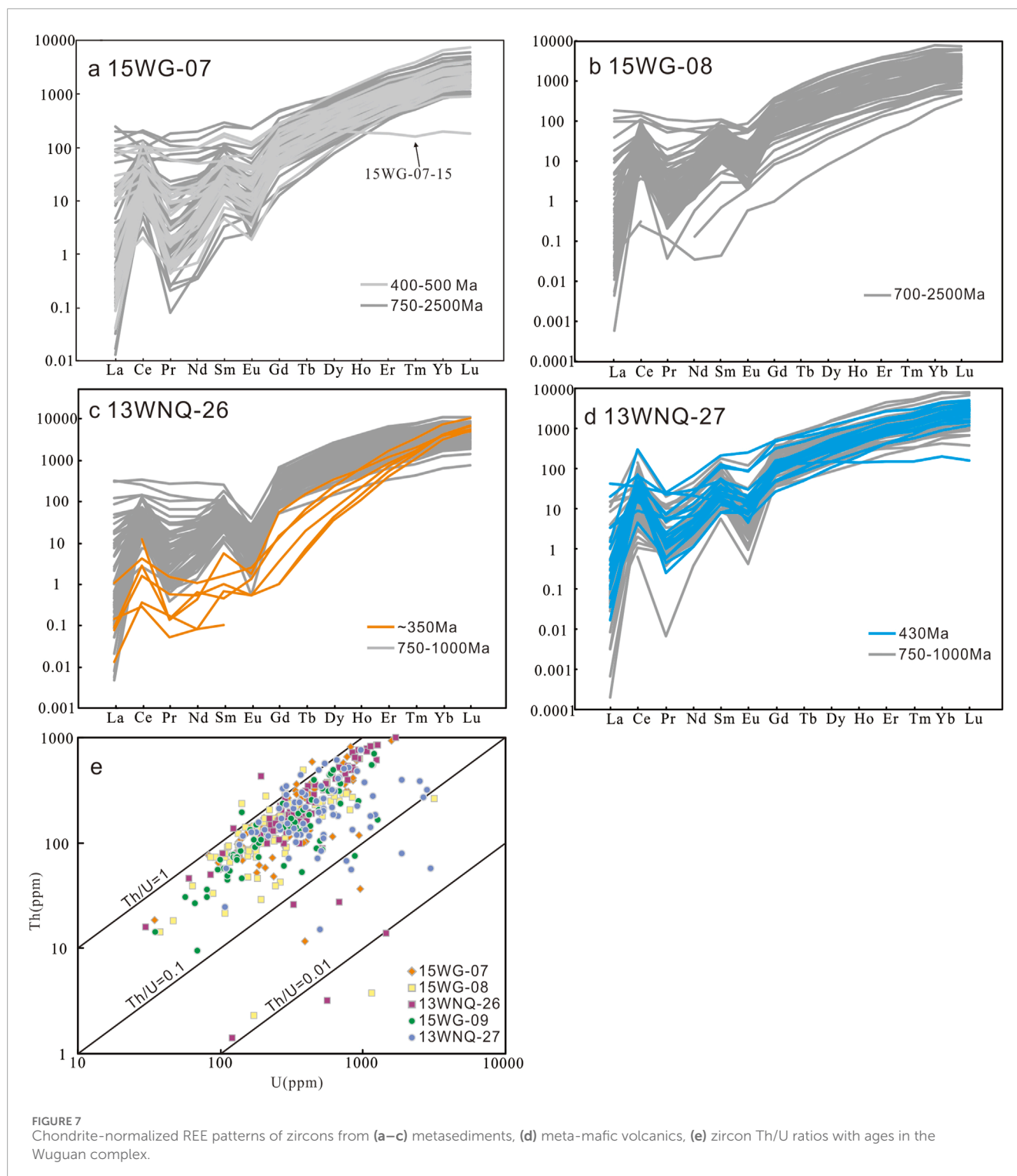
All amphibolites display very uniform chondrite-normalized REE patterns, with LREE weak enrichment relative to the HREE, weak positive Eu anomalies ($\text{Eu}/\text{Eu}^* = 0.94\text{--}1.24$) and moderate fractionation ($\text{La}_\text{N}/\text{Yb}_\text{N} = 3.17\text{--}5.59$) (Figure 9c). In the primitive mantle-normalized spider diagram (Figure 9d), the samples show no depletion of Nb and Ta, and exhibit significant positive Pb anomalies. The significant negative Sr anomalies in sample 13WNQ-27 are attributed to the incompatibility of Sr during hydrothermal alteration. All amphibolite exhibit both E-MORB-like and OIB-like trace elemental characteristics. Overall, the geochemical signatures suggest an intraplate tectonic setting or continental rift environment for the protolith basalts.

5 Discussion

5.1 Ages and depositional setting of meta-sedimentary rocks in the Wuguan Complex

5.1.1 Depositional age of meta-sedimentary rocks

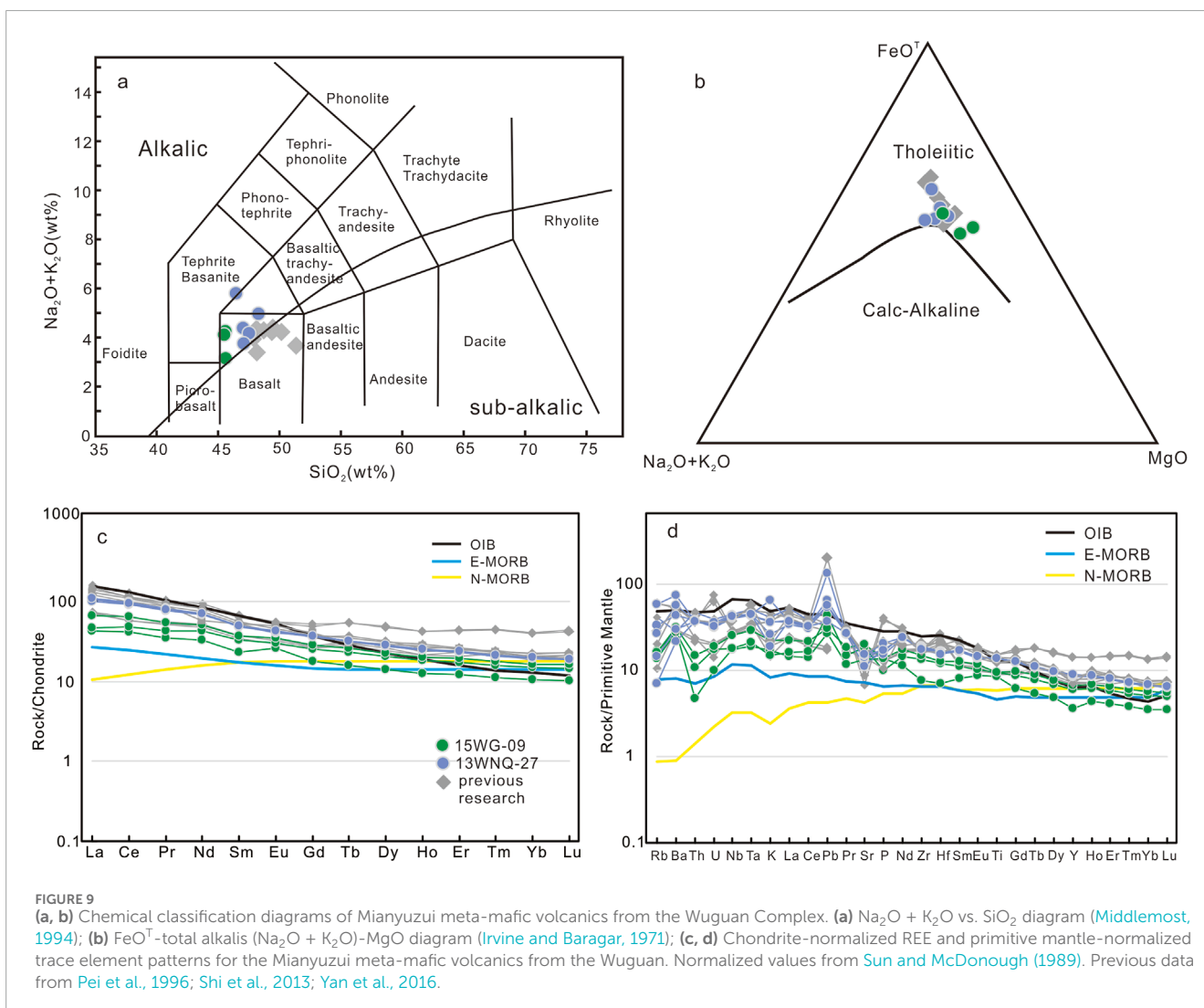
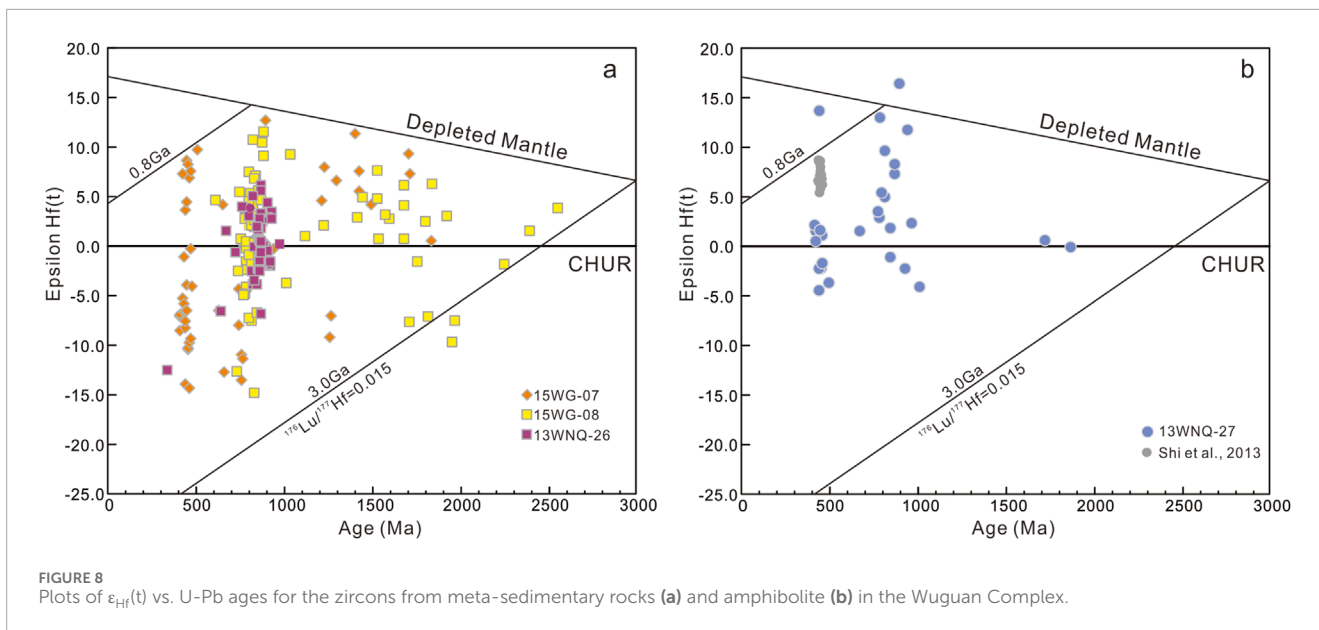
It is generally accepted that the youngest concordant age of detrital zircons from sedimentary rocks can be used to constrain the maximum depositional age (e.g., Fedo et al., 2003; Nelson, 2001; Williams, 2001). Furthermore, the youngest detrital zircon population is a robust indicator of depositional age only if coeval magmatism was ongoing (Dickinson and Gehrels, 2009). In this study, Sample 15WG-07 yields a youngest detrital age of ~ 410 Ma, indicating deposition in the Middle Devonian or slightly younger. The North Qinling belt contains widespread Early Paleozoic granitoids and related volcanic rocks (Zhang et al., 2013; Wang et al., 2003; Wang X.X. et al., 2013). These magmatic events, ranging through the Late Ordovician–Silurian ($\sim 450\text{--}420$ Ma),

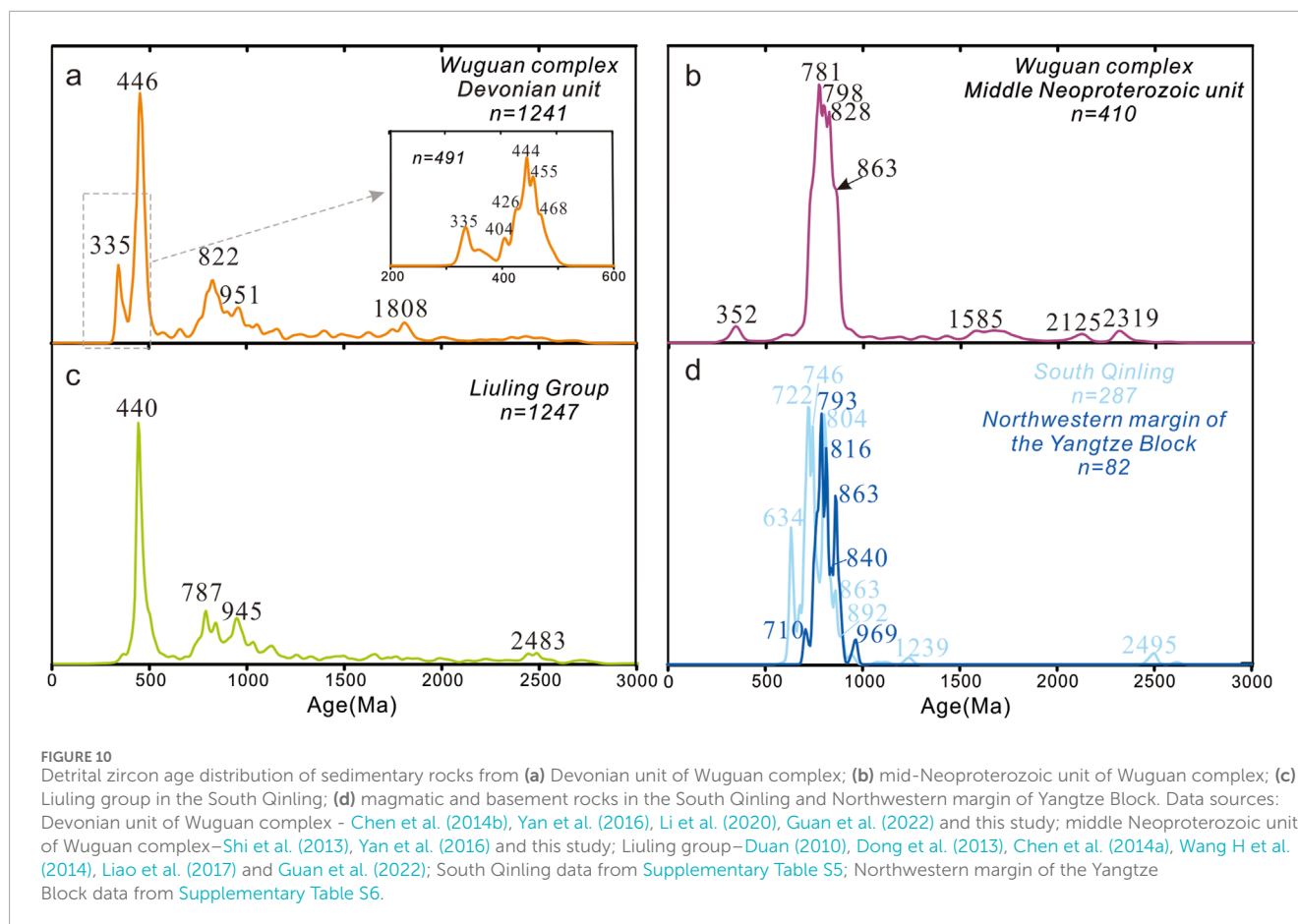


would have supplied young zircon grains to the sedimentary systems up to the early Devonian. Thus, the youngest detrital zircons in sample 15WG-07 yielding a mean of 410 ± 9 Ma are likely recording near-depositional ages. Similarly, samples 15WG-08 and 13WNQ-26 have youngest detrital ages ~ 746 – 748 Ma, suggesting a Mid-Neoproterozoic depositional age. These ages are significantly older than the regional metamorphic overprint (~ 340 – 310 Ma; Chen et al., 2020; Sheir et al., 2024; Bader et al.,

2025), confirming that sedimentation occurred well before the Late Paleozoic metamorphism.

Combining our data with previous detrital zircon ages from the Wuguan Complex (Chen et al., 2014a; Yan et al., 2016; Li et al., 2020; Guan et al., 2022), we identify two distinct types of detrital age patterns for the Wuguan metasedimentary rocks (Figures 10a, b). The first type is characterized by predominantly early Paleozoic ages with a prominent peak at ~ 446 Ma (Figure 10a). In this type,





and after excluding the clearly metamorphic zircon ages (e.g., 310–360 Ma in sample 13WNQ-26), the youngest detrital zircons in each sample range from ~438 Ma to ~380 Ma (Table 2; Figure 10a). The second type shows a youngest detrital zircon population at ~740–760 Ma (Table 2), significantly older than the first type, with a dominant age peak at ~650–900 Ma (Figure 10b), indicating deposition around 740 Ma. Based on these two distinct detrital age populations and youngest age peaks, the metasedimentary rocks of the Wuguan Complex can be subdivided into a Devonian unit and a Mid-Neoproterozoic unit.

It should be noted that this subdivision by age does not imply a perfectly separate stratigraphic sequence in the field. In fact, some meta-sedimentary rocks mapped within the Mid-Neoproterozoic unit contain detrital zircon age spectra similar to the Devonian unit (e.g., with ~440 Ma peaks), suggesting that the two units may be tectonically interleaved or in close proximity. Therefore, we use these age groups to inform a subdivision of the complex, but we emphasize that these units are tectonic slices in a *mélange* rather than laterally continuous stratigraphic units.

5.1.2 Provenance of detrital zircons in the meta-sedimentary rocks

The sediments eroded from orogenic belts and deposited in adjacent basins preserve valuable information about their provenance. Geochemical studies indicate that the Wuguan sedimentary protoliths had low compositional maturity and

were derived from proximal continental arc sources, dominated by felsic material with only minor mafic/ultramafic input (Yan et al., 2016). The sedimentary rocks of the Wuguan Complex predominantly composed of greywacke and lithic sandstone (Yan et al., 2016; Li et al., 2020) with minor Mg-Fe minerals (i.e., amphibole Figures 4a, b), suggesting that these deposits were likely formed close to the source. Thus, the provenance of the sedimentary protoliths most likely originated from adjacent continents, i.e., the North China Craton, the North Qinling belt, the South Qinling Belt and the Yangtze Block.

Detrital zircons from the Devonian unit display the dominant age population falls within the range of ca. 407–505 Ma, with two subordinate age clusters at ca. 632–896 Ma and ca. 1,191–1825 Ma (Figure 11c). These age spectra closely resemble the age pattern of Upper-Middle Devonian Liuling Group (Figure 10c), suggesting a common source and tectonic setting for these deposits. In contrast, detrital zircons from the middle Neoproterozoic unit show the most dominant age population is ca. 732–967 Ma, comprising 85% of all ages (Figure 11d). Widespread magmatic events between 650 and 900 Ma in the South Qinling and the northwestern margin of the Yangtze Block could have served as the source for these detrital zircons (Figure 10d).

A dominant age population between 400 and 505 Ma with an age peak at 440 Ma (Figure 10c), which are comparable to the episode of voluminous early Paleozoic magmatism in the North Qinling Belt (e.g., Wang C. et al., 2013; Zhang et al., 2013; Ren et al.,

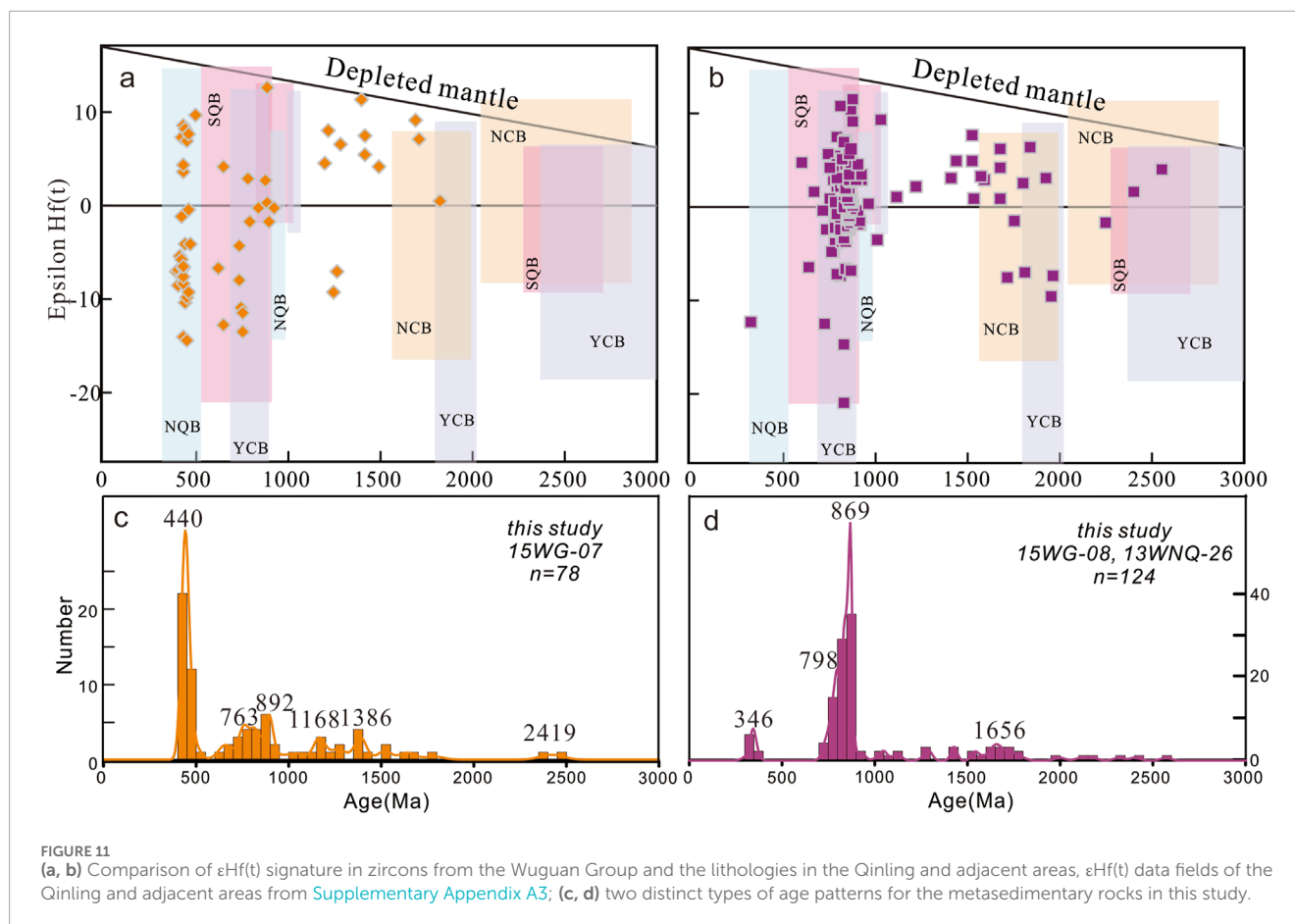
TABLE 2 The maximum depositional ages of rocks from the Wuguan Complex.

	Rock units	Lithology	The maximum depositional age (Ma)	References
Middle Neoproterozoic unit		Gneiss	736 ± 8	Shi et al. (2013)
	Maoping	Metamorphosed sandstone	554 ± 6	Yan et al. (2016)
	Balipo	Metamorphosed sandstone	650 ± 9	
	Maoping	Metapsammite	741 ± 4	this study
	Hualing		732 ± 6	
Devonian unit	Tieyupu	Metaquartzite	423 ± 5	Chen et al. (2014b)
	Diaozhuang	Mica-quartz schist	407 ± 3	this study
	Diaozhuang	Mica-quartz schist	433 ± 5	Yan et al. (2016)
	Balipo	Metamorphosed sandstone	427 ± 3	
	Maoping	Metamorphosed sandstone	403 ± 1	
			419 ± 3	
	Mianyuzui	Sandstone	483 ± 6	
			358 ± 3	
	Hualing	Greywacke	365 ± 5	
		Mica-quartz schist	407 ± 11.3	Li et al. (2020)
			412 ± 11	
			426 ± 11	
			371 ± 12	
Metasiltstone		376 ± 11		
		438 ± 13		
	Garnet staurolite mica schist	409 ± 12	Guan et al. (2022)	

2021). Further constraints on the nature of the magma sources can be inferred from the zircon Hf isotope compositions of these meta-sedimentary rocks. The early Paleozoic detrital zircons exhibit both negative and positive $\epsilon_{\text{Hf}}(t)$ values, with the majority showing negative values. This characteristic is similar to that observed in early Paleozoic magmatic rocks from the North Qinling Belt (Figure 11a).

Another predominant detrital zircon age population ranges between 632 and 896 Ma, with peaks at 822 Ma (Figure 10a). The 750–830 Ma detrital zircons are consistent with the ages of 640–810 Ma granitic and mafic intrusions in the South Qinling Belt (Figure 10d; Li H. K. et al., 2003; Ling et al., 2007; Zhang et al., 2016; Dong et al., 2017; 2024; Wu et al., 2024), as well as the voluminous Neoproterozoic magmatic rocks from the Bikou, Hannan, and Micangshan massifs along the northwestern margin of the Yangtze Block (Figure 10d; Dong et al., 2011c; Dong et al., 2012; Dong et al., 2024; Zhao and Zhou, 2009; Wang et al., 2012; Wu et al., 2024). Some researchers have proposed that the 750–850 Ma age population could be derived from eclogites and meta-mafic rocks of the Qinling

and Kuanping groups in the North Qinling Belt rather than the South Qinling Belt (Yan et al., 2016; Li et al., 2020; Zhao et al., 2021). However, the protolith of the eclogites and Neoproterozoic meta-mafic rocks from the Qinling Complex exhibits high positive zircon $\epsilon_{\text{Hf}}(t)$ values (Wang et al., 2011; Wang et al., 2013b; Yu et al., 2016). In contrast, the 750–890 Ma detrital zircons in this study contain 33% of grains with negative $\epsilon_{\text{Hf}}(t)$ values (−0.2 to −17.9; Figure 9), which are more similar to those of Neoproterozoic zircons from the Douling Group (−5.4 to −0.3; Shi et al., 2013; Zhang et al., 2018) and Liuba granites (−14.9 to −4.9; Zhang et al., 2016) in the South Qinling Belt (Figures 11a, b). Moreover, while the eclogites and meta-mafic rocks with protolith ages of ca. 750–850 Ma in the North Qinling Belt could have been a potential source for the Wuguan Complex, their limited outcrop area (less than 5% of the Qinling Complex) would not have been capable of providing the voluminous detritus in the Wuguan sediments. Compared to the widespread Neoproterozoic magmatic and sedimentary rocks in the South Qinling Belt and the northwestern margin of the Yangtze



Block, the small number of exposed mafic rocks from the North Qinling Belt is unlikely to be the main source of the Neoproterozoic detrital zircons (ca. 750–850 Ma) in the Wuguan sediments.

In addition, the paragneiss of the Qinling Complex in the North Qinling belt should be the main source of minor Mesoproterozoic–Archean detrital zircon population of the Wuguan Complex. Collectively, the sediments in the Devonian unit were largely derived from the North Qinling with minor contributions from the South Qinling belt and the northwestern Yangtze Block. Whereas, the Neoproterozoic zircons from the middle Neoproterozoic unit was only originated from the South Qinling and the northwestern margin of the Yangtze Block. These facts further supported previous interpretation that the Wuguan Complex is a lithological complex rather than a continuous lithostratigraphic unit (Pei et al., 1997; Yan et al., 2016; Chen et al., 2014a; 2020; Li et al., 2020).

5.2 Age and petrogenesis of meta-mafic volcanic rocks in the Wuguan Complex

5.2.1 Age of the protoliths

Mafic volcanic rocks are an important component of the Wuguan Complex, but there is ongoing debate regarding the age and tectonic significance of their protoliths. Pei et al. (1997) proposed that the protolith of the mafic volcanic rocks was Neoproterozoic, suggesting that they were rift-related basalts later incorporated into

the Wuguan mélange. Lu et al. (2004) suggested that the protolith formed at $1,243 \pm 46$ Ma (TIMS) and underwent metamorphism at 436 ± 46 Ma. In contrast, Chen et al. (2009) argued that the protolithic age of the amphibolite was no older than the late Devonian, with ca. 348 Ma metamorphism by zircon LA-ICP-MS dating. More recently, Chen et al. (2014b) and Sheir et al. (2024) reported the Silurian to early Devonian protolith age of 446 ± 2 Ma and ca. 405–425 Ma for garnet amphibolite and diabase dike in the Wuguan Complex. Shi et al. (2013) obtained zircon ages of ~ 440 Ma from an amphibolite and interpreted them as metamorphic ages, inferring an early Neoproterozoic (~ 800 Ma) protolith that was metamorphosed during the Silurian. They suggested these mafic rocks were emplaced into the Wuguan sedimentary prism in the latest Neoproterozoic to earliest Paleozoic, with the ~ 440 Ma ages reflecting Silurian metamorphism. However, CL imaging and high Th/U ratios (average ~ 1.06) of those zircons indicate a magmatic origin for the Early Paleozoic grains. We therefore suggest that the 444 ± 2 Ma age reported by Shi et al. (2013) likely represents the crystallization age of the basaltic protolith. In our study, amphibolite sample 13WNQ-27 yields a mean weighted U-Pb age of 436 ± 6 Ma, suggesting that its protolith formed during the Silurian. Combining these data, we propose that ~ 440 Ma is the best estimate for the formation age of the meta-mafic volcanic protoliths in the Wuguan Complex.

It is noteworthy that the U-Pb age spectrum of sample 13WNQ-27 (Figure 6d) exhibits multiple age populations, resembling those of

the metasedimentary rocks. There are two possibilities: (1) the $\sim 436 \pm 6$ Ma represents the crystallization age of the protolith (a Silurian mafic intrusion or flow) and the older zircons are xenocrysts picked up from continental crust or sediment during magma ascent; or (2) the amphibolite could be meta-volcanic or meta-volcaniclastic rock that contains detrital zircons from its depositional environment. Given the clear magmatic zoning and high Th/U values of the Silurian-age zircons in 13WNQ-27, we interpret ~ 436 Ma as the crystallization age of an igneous protolith (likely a basaltic flow or sill) that assimilated older crustal material or incorporated detrital zircons during emplacement. However, a volcanoclastic or sedimentary origin for the protolith cannot be entirely ruled out.

5.2.2 Petrogenesis of the protoliths

REEs, HFSEs such as Th, Nb, Ta, Zr, Hf, and Ti, and transitional metals like Sc, V, Cr, and Ni, are generally considered immobile during low-grade metamorphism and alteration (Gao et al., 1999; Polat and Hofmann, 2003). The amphibolite exhibits strong correlations between Hf, Ti, Ce, Yb, Nb, and Zr (Supplementary Appendix A2), suggesting that these elements remain relatively immobile during subsequent alteration and metamorphic processes. In contrast, LREEs such as Rb and Ba are scattered and no correlations with Zr, indicating varying degrees of mobility. Therefore, the subsequent discussion on tectonic significance will be primarily based on most of the immobile elements.

The amphibolite show sub-alkalic to alkaline basaltic bulk composition and a tholeiitic trend (Figures 9a, b). They display both MORB-like and OIB-like trace elemental characteristics (Figures 9c, d). On the Th/Yb versus Nb/Yb diagram, all meta-mafic volcanic rocks lie along the MORB-E-MORB-OIB array (subduction-unrelated field), consistent with an intraplate or oceanic within-plate basalt affinity (Figure 12a). Their combined enrichment in Nb–Ta and high TiO₂, yet with no indication of subduction-related enrichment in Th or LILEs, suggests they did not form in a typical arc or back-arc basin setting. Instead, the data point toward an intraplate tectonic environment, such as a continental rift or ocean island. The zircon populations provide additional constraints. As shown in Figure 6d, amphibolite contains numerous xenocrystal and/or inherited zircons with ages ranging from 600 Ma to 2,500 Ma. The significant time gap (up to 2000 Ma) between the crystallized age (ca. 410–440 Ma) and the oldest xenocrystal zircons ($\sim 2,500$ Ma) strongly suggests involvement of ancient continental material. In the Zr–Y–Nb and La–Nb–Y tectonic discrimination diagrams (Figures 12b, c), the amphibolites plot in the within-plate basalt field, supporting an intraplate setting. The high Ti content (TiO₂ up to 3.11 wt%) and Nb–Ta enrichment are characteristic of within-plate (plume-related) basalts. This interpretation is further supported by the depleted zircon $\epsilon_{\text{Hf}}(t)$ values (Figure 8b) indicating an enriched (possibly continental lithospheric) mantle source, and by field observations of these amphibolites occurring as lenses or dikes intruding sedimentary rocks and marbles (Figures 3e, f) rather than as a coherent oceanic crustal section. In addition, the geochemical traits of the Wuguan amphibolites differ from those of the Ordovician–Silurian arc basalts of the nearby Danfeng Complex, which have distinct arc-like signatures (Dong et al., 2011b). However, we note that

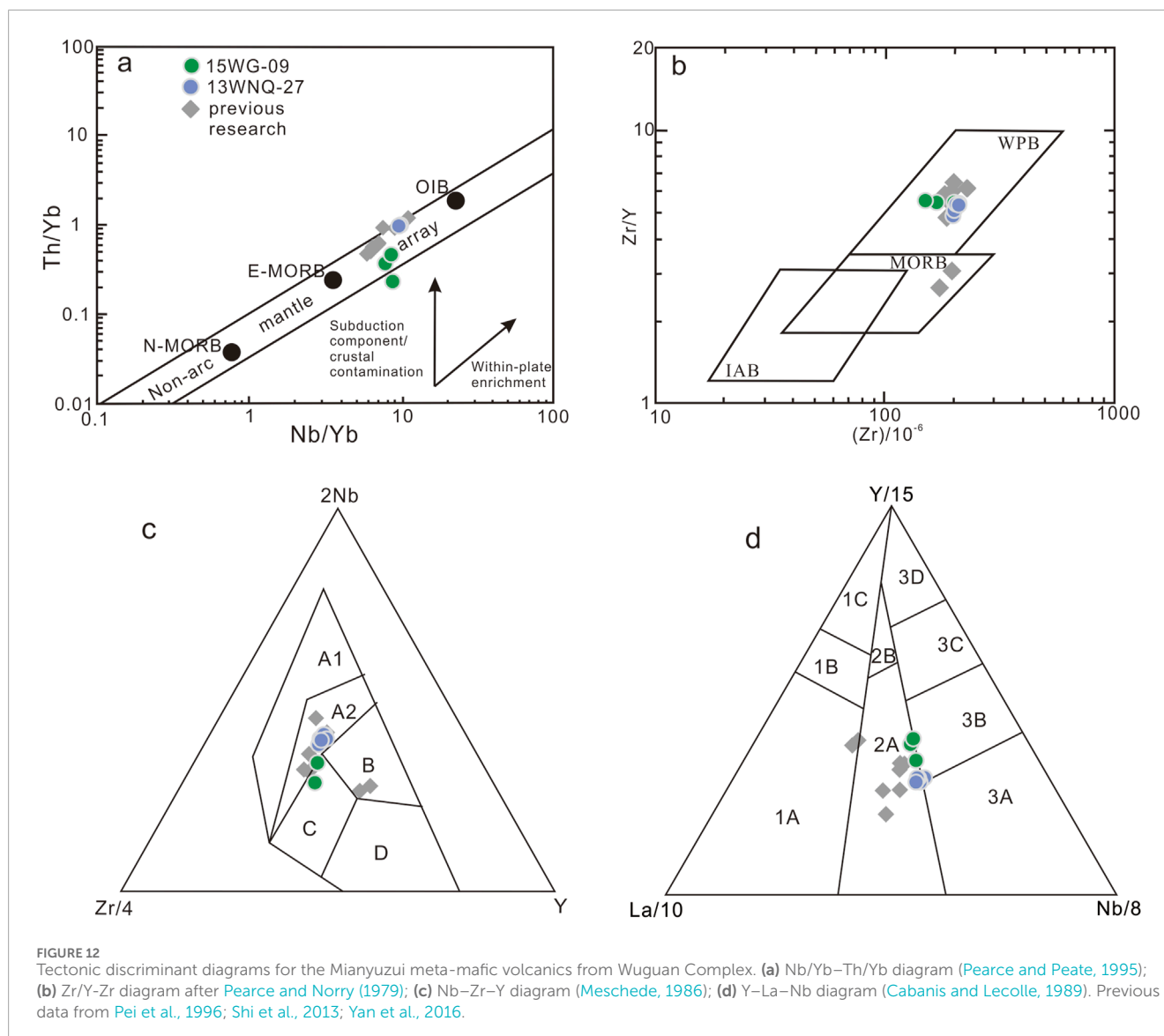
the presence of inherited ancient zircons in the Wuguan basalts does not entirely preclude an oceanic setting, as rare cases of oceanic basalts carrying recycled continental components have been documented (Liu et al., 2022).

Taken together, we infer that the Wuguan meta-mafic volcanic unit formed during the Silurian (~ 440 Ma) in an intraplate extensional setting. One plausible scenario is a local Silurian extensional event within the South Qinling margin (perhaps related to slab break-off or back-arc extension during an ongoing collision) that generated mafic magmatism. This is consistent with the absence of Silurian–Devonian shallow-marine strata in the South Qinling (Ren et al., 2019; Jiang et al., 2019) and with the occurrence of coeval mafic dikes intruding the Wuguan Complex to the west (Dong et al., 2013). We suggest that these basalts mark a brief tectonic transition from compression to extension in the South Qinling Belt during the Silurian.

5.3 Tectonic implications

Since Yu et al. (1988) presented Wuguan Complex as a forearc sedimentary prism, it has been generally accepted that the Wuguan Complex is a tectonic mélange rather than a continuous lithostratigraphic unit. However, its ages, provenance, and tectonic setting remain controversial, leaving its geological implications for the evolution of the Qinling Orogenic belt ambiguous. Pei et al. (1997) suggested that the meta-sedimentary and mafic-volcanic rocks in the Complex should be formed at Neoproterozoic in an active continental and within-plate setting, a view also supported by Lu et al. (2004) and Shi et al. (2013). Dong et al. (2013) reported the Silurian depositional age (ca. 455–435 Ma) for the forearc sedimentary prism in Heihe area, while the widespread Devonian sediments (i.e., Liuling Group) were deposited in a foreland basin, a passive margin or an extensive basin (e.g., Gao et al., 1995; Zhang et al., 2001; Dong et al., 2013; Liao et al., 2017; Ren et al., 2019). This evidence supports the closure of Paleo-Qinling Oceanic prior to the Devonian. In contrast, Yan et al. (2016) proposed that the Wuguan Complex comprises late Ordovician (ca. 520–460 Ma) island arc or E-MORB basalts, along with late Ordovician to early Silurian (ca. 450–430 Ma) and late Devonian to early Carboniferous (ca. 378–351 Ma) arc-related volcanic and sedimentary rocks. They interpreted the provenance of these components as being derived from a continental arc source in the North Qinling belt (Chen et al., 2014a; Yan et al., 2016; Li et al., 2020), suggesting that the Wuguan Complex was deposited in a fore-arc basin formed by the northward subduction of the long-lived Paleo-Qinling Ocean during at least ca. 400–330 Ma (Yan et al., 2016; Chen et al., 2020; Li et al., 2020; Bader et al., 2025).

The detrital zircons from the Wuguan metasedimentary rocks indicate two main depositional periods (Mid-Neoproterozoic and Devonian), confirming that the Wuguan Complex is not a single continuous sequence but a tectonic mélange of different-aged units. The Mid-Neoproterozoic sedimentary unit records clastic deposition on the northern margin of the Yangtze (South Qinling), while the Devonian unit corresponds to clastic deposition related to the convergence of the North and South China blocks. The Silurian mafic unit, with its intraplate basalt signature, points to a localized extensional regime in the midst of overall



convergence. We propose that a reappraisal of the Wuguan Complex that highlights three components, including Mid-Neoproterozoic metasedimentary slices, Silurian meta-mafic volcanic slices, and Devonian metasedimentary slices. These units were structurally juxtaposed by ductile strike-slip faults (Chen et al., 2014a; Jiang et al., 2017; Sheir et al., 2024; Bader et al., 2025) during the Early Carboniferous.

The Silurian meta-mafic volcanic unit (ca. 430–440 Ma) includes mafic flows interlayered with carbonate and clastic rocks. These intercalated marbles and sandstones in the Silurian unit can be interpreted as foredeep deposits along the southern edge of the North Qinling arc, coincident with mafic volcanism in an intraplate setting. This scenario indicates a local tectonic transition in the Qinling Belt from compressional to extensional during the Silurian. It is supported by (1) the presence of coeval (~435 Ma) mafic dikes intruding the Wuguan Complex in the Heihe area (Dong et al., 2013), and (2) the general absence of extensive Silurian–Devonian shallow marine strata in the South Qinling, where Late Paleozoic sediments lie unconformably on Early Paleozoic rocks, reflecting

a collisional orogenic event between the North and South Qinling that began in the Late Early Silurian and was largely complete by the Devonian (Jiang et al., 2019; Ren et al., 2019; Leng, 2023). The Devonian sedimentary unit shows detrital input largely from the North Qinling with minor contributions from the South Qinling, and is correlative with the Devonian Liuling Group, interpreted as a foreland or peripheral basin deposit formed after the main phase of Paleo-Qinling ocean closure (Gao et al., 1995; Zhang et al., 2001; Dong et al., 2013; Liao et al., 2017; Ren et al., 2019). However, other studies suggest that the Paleo-Qinling Ocean remained at least partially open through Devonian time, with subduction persisting until the Late Paleozoic (Yan et al., 2016; Chen et al., 2020; Li et al., 2020; Bader et al., 2025). In this scenario, the Devonian Wuguan Complex (and Liuling Group) could have formed in a subduction-related fore-arc or accretionary basin rather than exclusively in a post-collisional setting. These evidences suggest that the collision between the North and South Qinling along the Shangdan suture zone was underway by the Early Silurian (Mattauer et al., 1985; Gao et al., 1995; Zhang et al., 2001; Liu et al., 2016;

Ren et al., 2019; Dong et al., 2011b; 2013; 2021), or possibly as early as the Early Ordovician (Liu et al., 2016; Liao et al., 2017). At the same time, continued subduction in certain segments of the suture through Devonian–Carboniferous time (Yan et al., 2016; Chen et al., 2020; Li et al., 2020) implies that final closure of the Paleo-Qinling Ocean was a protracted, diachronous process.

6 Conclusion

- (1) The meta-sedimentary rocks in the Wuguan Complex can be subdivided into a Devonian (ca. 380–400 Ma) Unit and a mid-Neoproterozoic (732–743 Ma) Unit. The Devonian sediments exhibit a mixed source, primarily derived from both North Qinling and South Qinling magmatic and/or basement rocks. The mid-Neoproterozoic sediments are derived from the widespread Neoproterozoic South Qinling magmatic rocks.
- (2) The meta-mafic volcanic rocks in the Wuguan Complex, with interlayers of marble and sedimentary rocks, formed at 436 ± 6 Ma, exhibiting high TiO_2 content, both E-MORB and OIB features, and depleted zircon $\varepsilon_{\text{Hf}}(t)$ values, indicating formation within an intraplate tectonic setting.
- (3) The lithological units in the Wuguan Complex have been re-evaluated and include the mid-Neoproterozoic sedimentary unit, the Silurian meta-mafic volcanic unit, and the Devonian sedimentary unit. These units were structurally juxtaposed by ductile strike-slip faults during the Early Carboniferous. The closure of the Paleo-Qinling Ocean and the collision between the North and South China blocks began by the Early Silurian (possibly as early as the Ordovician), but subduction likely continued in parts of the orogen into the Devonian, indicating final closure of the Paleo-Qinling Ocean was a protracted, diachronous process.

Data availability statement

The original contributions presented in the study are included in the article/Supplementary Material, further inquiries can be directed to the corresponding author.

Author contributions

GW: Writing – original draft, Conceptualization, Data curation, Formal Analysis, Investigation, Methodology. XL: Writing – review and editing, Conceptualization, Data curation, Formal Analysis, Funding acquisition, Investigation, Methodology. LL: Writing – review and editing, Conceptualization, Funding acquisition,

Investigation. YW: Investigation, Writing – review and editing, Conceptualization, Data curation. WY: Formal Analysis, Writing – review and editing, Data curation, Investigation.

Funding

The author(s) declare that financial support was received for the research and/or publication of this article. This work was supported by funds from National Natural Science Foundation of China (Grant Nos 42030307 and 42272059).

Acknowledgments

We thank Dr. Zhian Bao for zircon Hf isotope analytical assistance, and thank Jinhong Liu, Yongsheng Gai and Sang Wan Pak for field work.

Conflict of interest

The authors declare that the research was conducted in the absence of any commercial or financial relationships that could be construed as a potential conflict of interest.

Generative AI statement

The author(s) declare that no Generative AI was used in the creation of this manuscript.

Publisher's note

All claims expressed in this article are solely those of the authors and do not necessarily represent those of their affiliated organizations, or those of the publisher, the editors and the reviewers. Any product that may be evaluated in this article, or claim that may be made by its manufacturer, is not guaranteed or endorsed by the publisher.

Supplementary material

The Supplementary Material for this article can be found online at: <https://www.frontiersin.org/articles/10.3389/feart.2025.1573681/full#supplementary-material>

References

- Bader, T., Ratschbacher, L., Franz, L., Romer, R. L., Zhang, L. F., de Capitani, C., et al. (2025). Carboniferous–triassic subduction in the Qinling orogen. *Gondwana Res.* 137, 171–208. doi:10.1016/j.gr.2024.09.015
- Bader, T., Ratschbacher, L., Franz, L., Yang, Z., Hofmann, M., Linnemann, U., et al. (2013). The Heart of China revisited, I. Proterozoic tectonics of the Qin mountains in the core of supercontinent Rodinia. *Tectonics* 32, 661–687. doi:10.1002/tect.20024
- Cabanis, B., and Lecolle, M. (1989). Le diagramme La/10–Y/15–Nb/8: un outil pour la discrimination des séries volcaniques et la mise en évidence des processus de mélange et/ou de contamination crustale. *Comptes Rendus l'Académie Sci. Série 2*, 2023–2029.
- Chen, D. L., Ren, Y. F., Gong, X. G., Liu, L., and Gao, S. (2015). Identification and its geological significance of eclogite in songshugou, the North Qinling. *Acta petrol. Sinica* 31 (7), 1841–1854.

- Chen, L. Y., Li, Y., Liu, X. C., Qu, W., and Hu, J. (2021). Deformational characteristics and geochronological constraints on the mianyuzui ductile shear zone. Eastern Qinling Area. *Acta Geosci. Sin.* 42, 13. doi:10.3975/cagsb.2020.042601
- Chen, L. Y., Liu, X. C., Qu, W., and Hu, J. (2014a). U-Pb zircon ages and geochemistry of the Wuguan complex in the Qinling orogen, central China: implications for the Late Paleozoic tectonic evolution between the Sino-Korean and Yangtze cratons. *Lithos* 192–195, 192–207. doi:10.1016/j.lithos.2014.01.014
- Chen, L. Y., Liu, X. C., Qu, W., and Hu, J. (2020). Metamorphic evolution and ⁴⁰Ar/³⁹Ar geochronology of the Wuguan complex, eastern Qinling area, China: implications for the late Paleozoic tectonic evolution of the Qinling orogen. *Lithos* 358–359, 105415. doi:10.1016/j.lithos.2020.105415
- Chen, L. Y., Luo, Y. L., Liu, X. C., Qu, W., and Hu, J. (2014b). U-Pb geochronology of detrital zircons from the Liuling Group and its tectonic significance. *Geol. Bull. China* 33 (9), 1363–1378.
- Chen, N. S., Ba, J., Zhang, L., Su, W., Liu, J. B., and Guo, S. (2009). Zircon LA-ICP-MS U-Pb dating of the wuguan group, shangdan fault zone, eastern qinling, China. *Geol. Bull. China* 28 (5), 556–560.
- Chen, Z. H., Lu, S. N., Li, H. K., Li, H. M., Xiang, Z. Q., Zhou, H. Y., et al. (2006). Constraining the role of the Qinling orogen in the assembly and break-up of Rodinia: tectonic implications for Neoproterozoic granite occurrences. *J. Asian Earth Sci.* 28, 99–115. doi:10.1016/j.jseae.2005.03.011
- Cui, Z., Sun, Y., and Wang, X. (1995). The discovery of radiolarians in the Danfeng ophiolite belt of the Qinling Mountains and its geological significance. *Sci. Bull.* 18, 1686–1688.
- Dickinson, W. R., and Gehrels, G. E. (2009). Use of U–Pb ages of detrital zircons to infer maximum depositional ages of strata: a test against a Colorado Plateau Mesozoic database. *Earth Planet. Sci. Lett.* 288, 115–125. doi:10.1016/j.epsl.2009.09.013
- Dong, Y., Hui, B., Sun, S., He, D., Sun, J., Zang, F., et al. (2024). Neoproterozoic tectonic evolution and proto-basin of the Yangtze Block, China. *Earth-Sci. Rev.* 249, 104669. doi:10.1016/j.earscirev.2023.104669
- Dong, Y., Neubauer, F., Genser, J., Sun, S., Yang, Z., Zhang, F., et al. (2018). Timing of orogenic exhumation processes of the Qinling Orogen: evidence from ⁴⁰Ar/³⁹Ar dating. *Tectonics* 37, 4037–4067. doi:10.1029/2017tc004765
- Dong, Y., Sun, S., Santosh, M., Zhao, J., Sun, J., He, D., et al. (2021). Central China orogenic belt and amalgamation of east asian continents. *Gondwana Res.* 100, 131–194. doi:10.1016/j.gr.2021.03.006
- Dong, Y. P., Liu, X. M., Neubauer, F., Zhang, G. W., Tao, N., Zhang, Y. G., et al. (2013). Timing of Paleozoic amalgamation between the North China and South China Blocks: evidence from detrital zircon U-Pb ages. *Tectonophysics* 586, 173–191. doi:10.1016/j.tecto.2012.11.018
- Dong, Y. P., Liu, X. M., Santosh, M., Chen, Q., Zhang, X. N., Li, W., et al. (2012). Neoproterozoic accretionary tectonics along the northwestern margin of the Yangtze Block, China: constraints from zircon U-Pb geochronology and geochemistry. *Precamb. Res.* 196–197, 247–274. doi:10.1016/j.precamres.2011.12.007
- Dong, Y. P., Liu, X. M., Santosh, M., Zhang, X. N., Chen, Q., Yang, C., et al. (2011c). Neoproterozoic subduction tectonics of the northwestern Yangtze Block in South China: constraints from zircon U-Pb geochronology and geochemistry of mafic intrusions in the Hannan Massif. *Precamb. Res.* 189, 66–90. doi:10.1016/j.precamres.2011.05.002
- Dong, Y. P., and Santosh, M. (2016). Tectonic architecture and multiple orogeny of the qinling orogenic belt, Central China. *Gondwana Res.* 29, 1–40. doi:10.1016/j.gr.2015.06.009
- Dong, Y. P., Sun, S. S., Yang, Z., Liu, X. M., Zhang, F. F., Li, W., et al. (2017). Neoproterozoic subduction-accretionary tectonics of the South qinling belt, China. *Precambrian Res.* 293, 73–90. doi:10.1016/j.precamres.2017.02.015
- Dong, Y. P., Zhang, G. W., Hauzenberger, C., Neubauer, F., Yang, Z., and Liu, X. M. (2011b). Palaeozoic tectonics and evolutionary history of the Qinling orogen: evidence from geochemistry and geochronology of ophiolite and related volcanic rocks. *Lithos* 122, 39–56. doi:10.1016/j.lithos.2010.11.011
- Dong, Y. P., Zhang, G. W., Neubauer, F., Liu, X. M., Genser, J., and Hauzenberger, C. (2011a). Tectonic evolution of the Qinling orogen, China: review and synthesis. *J. Asian Earth Sci.* 41, 213–237. doi:10.1016/j.jseae.2011.03.002
- Duan, L. (2010). Detrital zircon provenance of the Silurian and Devonian in South Qinling, and the northwestern margin of Yangtze terrane and its tectonic implications. (master's thesis.) Northwest University, Xi'an, China.
- Fedo, C. M., Sircombe, K. N., and Rainbird, R. H. (2003). Detrital zircon analysis of sedimentary record. *Rev. Mineral. Geochem., Mineral. Soc. Am. Geochem. Soc.*, 277–303. doi:10.2113/0530277
- Gao, S., Ling, W. L., Qiu, Y. M., Lian, Z., Hartmann, G., and Simon, K. (1999). Contrasting geochemical and Sm-Nd isotopic compositions of Archean metasediments from the Kongling high-grade terrain of the Yangtze craton: evidence for cratonic evolution and redistribution of REE during crustal anatexis. *Geochim. Cosmochim. Acta* 63, 2071–2088. doi:10.1016/s0016-7037(99)00153-2
- Gao, S., Zhang, B. R., Gu, X. M., Xie, X. L., Gao, C. L., and Guo, X. M. (1995). Silurian–devonian provenance changes of South Qinling basins: implications for accretion of the Yangtze (South China) to the North China cratons. *Tectonophysics* 250, 183–197. doi:10.1016/0040-1951(95)00051-5
- Gong, X. K., Chen, D. L., Ren, Y. F., Liu, L., Gao, S., and Yang, S. J. (2016). Identification of coesite-bearing amphibolite in the North Qinling and its geological significance. *Chin. Sci. Bull.* 61 (12), 1365–1378. doi:10.1360/n972015-01277
- Guan, M., Li, J. H., Jia, G. Q., Ren, S. L., and Song, C. Z. (2022). U–Pb zircon ages and geochemistry of the wuguan complex and liuling group: implications for the late paleozoic tectonic evolution of the qinling orogenic belt, Central China. *Minerals* 12, 1026. doi:10.3390/min12081026
- Hacker, B. R., Ratschbacher, L., and Liou, J. G. (2004). Subduction, collision and exhumation in the ultrahigh-pressure Qinling-Dabie orogen. *J. Geol. Soc. Lond.* 226, 157–175. doi:10.1144/gsl.sp.2004.226.01.09
- He, Z. J., Niu, B. G., and Ren, J. S. (2005). Tectonic discriminations of sandstones geochemistry from the middle-late devonian liuling group in Shanyang area, southern shaanxi. *Chin. J. Geol.* 40, 594–607.
- Hu, J., Liu, X. C., Chen, L. Y., Qu, W., Li, H. K., and Geng, J. Z. (2013). A 2.5 Ga magmatic event at the northern margin of the Yangtze craton: evidence from U-Pb dating and Hf isotopic analysis of zircons from the Douling Complex in the South Qinling orogen. *Chin. Sci. Bull.* 28–29, 3564–3579. doi:10.1007/s11434-013-5904-1
- Irvine, T. N., and Baragar, W. R. A. (1971). A guide to the chemical classification of the common volcanic rocks. *Can. J. Earth Sci.* 8, 523–548. doi:10.1139/e71-055
- Jiang, X. J., Ren, J. S., Zhou, D. W., Zhao, L., Liu, R. Y., and Sun, H. Y. (2019). The caledonian tectonic-sedimentary evolution process in eastern qinling orogenic belt. *Earth Sci.* 44 (1), 88–108. doi:10.3799/dqkx.2018.281
- Jiang, Y. Y., Xiong, H., and Zhang, Z. M. (2017). Metamorphic P-T path and tectonic implication of garnet-biotite schist of the Wuguan complex, Qinling orogen. *Acta Petrol. Sin.* 33 (8), 2563–2574.
- Leng, Y. X. (2023). “Geochemical and geochronological characteristics of paleozoic sedimentary rocks in the southern qinling orogenic belt,” in *Its tectonic implications*[D]. Beijing: China University of Geosciences.
- Li, H. K., Lu, S. N., Chen, Z. H., Xiang, Z. Q., Zhou, H. Y., and Hao, G. J. (2003b). Zircon U-Pb geochronology of rift-type volcanic rocks of the Yaolinghe Group in the South Qinling orogen. *Geol. Bull. China* 22 (10), 775–781.
- Li, J. H., Lan, R. X., Ren, S. L., Song, C. Z., and Li, L. M. (2020). Subduction and collision processes between the North China and South China blocks constrained by the geochronology and geochemistry of the Wuguan Complex in the Qinling orogen. China. *Int. Geol. Rev.* 62, 1538–1554. doi:10.1080/00206814.2019.1658231
- Li, Y., Yang, J. S., Dilek, Y., Zhang, J., Pei, X. Z., Chen, S. Y., et al. (2015). Crustal architecture of the Shangdan suture zone in the early Paleozoic Qinling orogenic belt, China: record of subduction initiation and backarc basin development. *Gondwana Res.* 27, 733–744. doi:10.1016/j.gr.2014.03.006
- Li, Z. X., Li, X. H., Kinny, P. D., Wang, J., Zhang, S., and Zhou, H. (2003a). Geochronology of Neoproterozoic syn-rift magmatism in the Yangtze Craton, South China and correlations with other continents: evidence for a mantle superplume that broke up Rodinia. *Precamb. Res.* 122, 85–109. doi:10.1016/S0301-9268(02)00208-5
- Liao, X. Y., Liu, L., Wang, Y. W., Cao, Y. T., Chen, D. L., and Dong, Y. (2016). Multi-stage metamorphic evolution of retrograde eclogite with a granulite-facies overprint in the Zhaigang area of the North Qinling Belt, China. *Gondwana Res.* 30, 79–96. doi:10.1016/j.gr.2015.09.012
- Liao, X. Y., Wang, Y.-W., Liu, L., Wang, C., and Santosh, M. (2017). Detrital zircon U-Pb and Hf isotopic data from the Liuling Group in the South Qinling belt: provenance and tectonic implications. *J. Asian Earth Sci.* 134, 244–261. doi:10.1016/j.jseae.2016.11.020
- Ling, W. L., Duan, R. C., Liu, X. M., Cheng, J. P., Mao, X. W., Peng, L. H., et al. (2010). U-Pb dating of detrital zircons from the Wudangshan Group in the South Qinling and its geological significance. *Chin. Sci. Bull.* 55, 2440–2448. doi:10.1007/s11434-010-3095-6
- Ling, W. L., Ren, B. F., Duan, R. C., Liu, X. M., Mao, X. W., and Peng, L. H. (2007). Zircon U-Pb isotopic geochronology of Wudangshan Group, Yaolinghe Group and basic intrusions and its geological significance. *Chin. Sci. Bull.* 52 (12), 1445–1456. doi:10.1007/s11434-008-0269-6
- Liu, C.-Z., Dick, H. J. B., Mitchell, R. N., Wei, W., Zhang, Z.-Y., Hofmann, A. W., et al. (2022). Archean cratonic mantle recycled at a mid-ocean ridge. *Sci. Adv.* 8 (22), eabn6749. doi:10.1126/sciadv.abn6749
- Liu, G. H., Zhang, S. G., and You, Z. D. (1993). *Metamorphic rocks in qinling orogen belt and its metamorphic evolution*. Beijing, China: Geology Press, 21 [in Chinese with English abstract].
- Liu, L., Liao, X. Y., Wang, Y. W., Wang, C., Santosh, M., Yang, M., et al. (2016). Early Paleozoic tectonic evolution of the North Qinling Orogenic Belt in Central China: insights on continental deep subduction and multiphase exhumation. *Earth-Sci. Rev.* 159, 58–81. doi:10.1016/j.earscirev.2016.05.005
- Liu, L., Liao, X. Y., Zhang, C. L., Chen, D. L., Gong, X. K., and Kang, L. (2013). Multi metamorphic timings of HP-UHP rocks in the North Qinling and their geological implications. *Acta Petrol. Sin.* 29, 1634–1656.

- Liu, R. Y., Niu, B. G., He, Z. J., and Ren, J. S. (2011). LA-ICP-MS zircon U-Pb geochronology of the eastern part of the Xiaomaoling composite intrusives in Zhushui area, Shanshan, China. *Geol. Bull. China* 30 (2/3), 448–460.
- Lu, S. N., Chen, Z. H., Li, H. K., Hao, G. J., Zhou, H. Y., and Xiang, Z. Q. (2004). Late Mesoproterozoic-early neoproterozoic evolution of qinling orogen. *Geol. Bull. China* 02, 107–112.
- Lu, S. N., Li, H. K., Chen, Z. H., Hao, G. J., Zhou, H. Y., Guo, J. J., et al. (2003). *Meso-neoproterozoic geological evolution of the qinling and its response to rodinia event*. Beijing: Geological Publishing House, 1–194.
- Lu, S. N., Yu, H. F., Li, H. K., Chen, Z. H., Wang, H. C., and Zhang, C. L. (2009). Precambrian geology of the west and Middle Central China orogen. *Geol. Publ. House* 76, 98. doi:10.3969/j.issn.1671-2552.2006.12.004
- Mattauer, M., Mattle, P., Malavieille, J., Tapponnier, P., Maslowski, H., Xu, Z. Q., et al. (1985). Tectonics of qinling belt: build-up and evolution of eastern asia. *Nature* 317, 496–500. doi:10.1038/317496a0
- Meng, Q. R. (1994). “Late paleozoic sedimentation,” in *Basin development and tectonics of the qinling orogenic belt*. Xi'an: Northwest University, 1–172.
- Meng, Q. R. (2017). Origin of the qinling mountains. *Sci. Sin. Terrae* 47, 412–420. doi:10.1360/n072016-00422
- Meng, Q. R., and Zhang, G. W. (2000). Geologic framework and tectonic evolution of the Qinling orogen, central China. *Tectonophysics* 323, 183–196. doi:10.1016/S0040-1951(00)00106-2
- Meschede, M. (1986). A method of discriminating between different types of mid-ocean ridge basalts and continental tholeiites with the Nb 1bZr 1bY diagram. *Chem. Geol.* 56, 207–218. doi:10.1016/0009-2541(86)90004-5
- Middlemost, E. K. (1994). Naming materials in the magma/igneous rock system. *Earth Sci. Rev.* 37, 215–224. doi:10.1016/0012-8252(94)90029-9
- Nelson, D. R. (2001). An assessment of the determination of depositional ages for precambrian clastic sedimentary rocks by U–Pb dating of detrital zircons. *Sediment. Geol.* 141–142, 37–60. doi:10.1016/S0037-0738(01)00067-7
- Nie, H., Yao, J., Wan, X., Zhu, X. Y., Siebel, W., and Chen, F. K. (2016). Pre cambrian tectonothermal evolution of South Qinling and its affinity to the Yangtze Block: evidence from zircon ages and Hf–Nd isotopic compositions of basement rocks. *Precambrian Res.* 286, 167–179. doi:10.1016/j.precamres.2016.10.005
- Niu, B. G., He, Z. J., Ren, J. S., Wang, J., and Deng, P. (2006). SHRMP U–Pb ages of zircons from the intrusions in the western Douling-Xiaomaoling uplift and their geological significances. *Geol. Rev.* 52, 826–835.
- Pearce, J. A., and Norry, M. J. (1979). Petrogenetic implications of Ti, Zr, Y and Nb variations in volcanic rocks. *Contributions Mineralogy Petrology* 69, 33–47. doi:10.1007/bf00375192
- Pearce, J. A., and Peate, D. W. (1995). Tectonic implications of the composition of volcanic arc magmas. *Annu. Rev. Earth Planet. Sci.* 23, 251–285. doi:10.1146/annurev.earth.23.1.251
- Pei, X. Z., Li, H. M., Li, G. G., Gao, D. X., Zhang, W. J., Wang, Q. Q., et al. (1996). *Geological mapping and report of Qingyouhe (I49E015011) and shangnan (I49E015012), 1:50000*
- Pei, X. Z., Li, H. M., Li, G. G., Zhang, W. J., Wang, Q. Q., and Li, Z. C. (1997). Sm–Nd age and geological significance of amphibolite of the Wuguan group complex on the southern side of the Shangdan fault zone in the east Qinling mountains. *Chin. Reg. Geol.* (01), 39–43.
- Pei, X. Z., Li, Z. C., Ding, S. P., Li, Y., Hu, B., and Liu, H. B. (2005). Geochemical characteristics and zircon U–Pb ages of island-arc basic igneous complexes in the Tianshui area, West Qinling. *Geol. China* 32 (4), 529–540.
- Polat, A., and Hofmann, A. W. (2003). Alteration and geochemical patterns in the 3.7–3.8 Ga Isua greenstone belt, West Greenland. *West Greenl.* 126, 197–218. doi:10.1016/S0301-9268(03)00095-0
- Ratschbacher, L., Hacker, B. R., Calvert, A., Webb, L. E., Grimmer, J. C., McWilliams, M. O., et al. (2003). Tectonics of the Qinling (Central China): tectonostratigraphy, geochronology, and deformation history. *Tectonophysics* 366, 1–53. doi:10.1016/S0040-1951(03)00053-2
- Ren, J., Zhu, J., Li, C., and Liu, R. (2019). Is the Qinling orogenic belt an Indosinian collision orogenic belt? *Earth Sci.* 44 (5), 1476–1486. doi:10.3799/dqkx.2019.047
- Ren, L., Liang, H. Y., Bao, Z. W., and Huang, W. T. (2021). Early Paleozoic magmatic “flare-ups” in western Qinling orogeny, China: new insights into the convergence history of the North and South China Blocks at the northern margin of Gondwana. *Lithos* 380–381, 105833. doi:10.1016/j.lithos.2020.105833
- Sheir, F., Li, W., Zhang, L., Baz, S., Jiang, L. Q., Liang, L., et al. (2024). Structural styles and chronological sequence of the Mianyuzui ductile strike-slip fault along the Shangdan suture Zone: implications for the Paleozoic tectonic evolution of the Qinling Orogenic Belt, China. *J. Asian Earth Sci.* 268, 106163. doi:10.1016/j.jseas.2024.106163
- Shi, Y., Yu, J. H., and Santosh, M. (2013). Tectonic evolution of the Qinling orogenic belt, Central China: new evidence from geochemical, zircon U–Pb geochronology and Hf isotopes. *Precamb. Res.* 231, 19–60. doi:10.1016/j.precamres.2013.03.001
- Sun, S. S., and McDonough, W. F. (1989). “Chemical and isotopic systematics of oceanic basalts: Implications for mantle composition and processes,” in *Magmatism in the Ocean Basins: Geological Society*. Editor A. D. Saunders, and M. J. Norry (London: Special Publication), 313–345. doi:10.1144/GSL.SP.1989.042.01.19
- Wang, C., Liu, L., Yang, W. Q., Cao, Y. T., Zhu, X. H., Chen, S. F., et al. (2013a). Provenance and ages of the altnyn complex in altnyn tagh: implications for the early neoproterozoic evolution of northwestern China. *Precamb. Res.* 230, 193–208. doi:10.1016/j.precamres.2013.02.003
- Wang, H., Wu, Y. B., Gao, S., Liu, X. C., Gong, H. J., Li, Q. L., et al. (2011). Eclogite origin and timings in the North Qinling terrane, and their bearing on the amalgamation of the South and North China Blocks. *J. Metamorph. Geol.* 29, 1019–1031. doi:10.1111/j.1525-1314.2011.00955.x
- Wang, H., Wu, Y. B., Gao, S., Liu, X. C., Liu, Q., Qin, Z. W., et al. (2013b). Continental origin of eclogites in the North Qinling terrane and its tectonic implications. *Res.* 230, 13–30. doi:10.1016/j.precamres.2012.12.010
- Wang, H., Wu, Y. B., Gao, S., Zheng, J. P., Liu, Q., Liu, X. C., et al. (2014a). Deep subduction of continental crust in accretionary orogen: evidence from U–Pb dating on diamond-bearing zircons from the Qinling orogen, central China. *Lithos* 190–191, 420–429. doi:10.1016/j.lithos.2013.12.021
- Wang, T., Wang, X. X., Zhang, G. W., Pei, X. Z., and Zhang, C. L. (2003). Remnants of a Neoproterozoic collisional orogenic belt in the core of the Phanerozoic Qinling orogenic belt (China). *Gondwana Res.* 4, 815–836. doi:10.1016/S1342-937X(05)71018-2
- Wang, W., Liu, S. W., Feng, Y. G., Li, Q. G., Wu, F. H., Wang, Z. Q., et al. (2012). Chronology, petrogenesis and tectonic setting of the Neoproterozoic Tongchang dioritic pluton at the northwestern margin of the Yangtze Block: constraints from geochemistry and zircon U–Pb–Hf isotopic systematics. *Gondwana Res.* 22 (2), 699–716. doi:10.1016/j.gr.2011.11.015
- Wang, X. X., Wang, T., and Zhang, C. L. (2013c). Neoproterozoic, Paleozoic, and Mesozoic granitoid magmatism in the Qinling Orogen, China: constraints on orogenic process. *J. Asian Earth Sci.* 72, 129–151. doi:10.1016/j.jseas.2012.11.037
- Wang, Y. Y., Pei, X. Z., Liu, C. J., Li, R. B., Li, Z. C., Wei, B., Ren, H. Z., et al. (2014). Detrital zircon LA-ICP-MS U–Pb ages of the Devonian Shujiaba Group in Shujiaba area of the West Qinling tectonic zone: constraints on material source and sedimentary age. *Geol. Bull. China* 33 (7), 1015–1027.
- Williams, I. S. (2001). Response of detrital zircon and monazite, and their U–Pb isotopic systems, to regional metamorphism and host-rock partial melting, Cooma Complex, southeastern Australia. *Aust. J. Earth Sci.* 48, 557–580. doi:10.1046/j.1440-0952.2001.00883.x
- Wu, P., Wu, Y. B., Zhang, S. B., Zheng, Y. F., Li, L., Gao, Y., et al. (2024). Revisiting neoproterozoic tectono-magmatic evolution of the northern margin of the Yangtze block, South China. *Earth Sci. Rev.* 255, 104825. doi:10.1016/j.earscirev.2024.104825
- Wu, Y. B., and Zheng, Y. F. (2013). Tectonic evolution of a composite collision orogen: an overview on the Qinling–Tongbai–Hong’an–Dabie–Sulu orogenic belt in central China. *Gondwana Res.* 23, 1402–1428. doi:10.1016/j.gr.2012.09.007
- Xia, L. Q., Xia, Z. C., Li, X. M., Ma, Z. P., and Xu, X. Y. (2008). Petrogenesis of the Yaolinghe Group, Yunxi Group, Wudangshan Group volcanic rocks and basic dyke swarms from eastern part of the south Qinling mountains. *Northwest. Geol.* 41, 1–29.
- Xu, Z., Li, Y., Ji, S., Li, G., Pei, X., Ma, X., et al. (2020). Qinling gneiss domes and implications for tectonic evolution of the Early Paleozoic Orogen in Central China. *J. Asian Earth Sci.* 188, 104052. doi:10.1016/j.jseas.2019.104052
- Yan, Z., Fu, C. L., Wang, Z. Q., Yan, Q. R., Chen, L., and Chen, J. L. (2016). Late Paleozoic subduction–accretion along the southern margin of the North Qinling terrane, central China: evidence from zircon U–Pb dating and geochemistry of the Wuguan Complex. *Gondwana Res.* 31. doi:10.1016/j.gr.2015.05.005
- Yan, Z., Wang, Z., Wang, T., Yan, Q., Xiao, W., Li, J., et al. (2007). Tectonic setting of Devonian sediment s in the Qinling orogen: constraints from detrital modes and geochemistry of clastic rocks. *Acta Petrol. Sin.* 23, 1023–1042.
- Yan, Z., Wang, Z. Q., Yan, Q. R., Wang, T., and Guo, X. Q. (2012). Geochemical constraints on the provenance and depositional setting of the Devonian Liuling Group, East Qinling Mountains, central China: implications for the tectonic evolution of the Qinling orogenic belt. *J. Sediment. Res.* 82, 9–20. doi:10.2110/jsr.2012.4
- Yang, J. S., Xu, Z. Q., Dobrzynetska, L. F., Green, H. W., Shi, R. D., Wu, C. L., et al. (2003). Discovery of metamorphic diamonds in central China: an indication of a >4000-km-long zone of deep subduction resulting from multiple continental collisions. *Terra nova.* 15, 370–379. doi:10.1046/j.1365-3121.2003.00511.x
- Yu, H., Zhang, H. F., Li, X. H., Zhang, J., Santosh, M., Yang, Y. H., et al. (2016). Tectonic evolution of the North Qinling Orogen from subduction to collision and exhumation: evidence from zircons in metamorphic rocks of the Qinling Group. *Gondwana Res.* 30, 65–78. doi:10.1016/j.gr.2015.07.003
- Yu, Z. P., and Meng, Q. R. (1995). Late Paleozoic sedimentary and tectonic evolution of the Shangdan suture, eastern Qinling, China. *J. SE Asian Earth Sci.* 11, 237–242. doi:10.1016/0743-9547(95)98084-F

- Yu, Z. P., Sun, Y., and Zhang, G. (1988). "The forearc sedimentary system in the Danfeng area, the Qinling Mountains," in *Formation and evolution of the qinling orogen*. Editor G. Zhang (Xi'an: Northwest University Press), 75–85.
- Zhang, C. L., Liu, L., Wang, T., Wang, X. X., Li, L., Gong, Q. F., et al. (2013). Granitic magmatism related to early Paleozoic continental collision in North Qinling. *Chin. Sci. Bull.* 35, 4405–4410. doi:10.1007/s11434-013-6064-z
- Zhang, G. W., Sun, Y., Yu, Z. P., and Xue, F. (1988). "The ancient active continental margin of the northern Qinling orogenic belt," in *Formation and evolution of the qinling orogen*. Editor G. W. Zhang (Xi'an: Northwest University Press), 48–64.
- Zhang, G. W., Zhang, B. R., Yuan, X. C., and Xiao, Q. H. (2001). *Qinling orogenic belt and continental dynamics*. Beijing: Science Press, 1–855.
- Zhang, G. W., Zhang, Z. Q., and Dong, Y. P. (1995a). Nature of main tectonic lithostratigraphic units of Qinling orogen: implications for the tectonic evolution. *Acta Petrol. Sin.* 11 (2), 101–114.
- Zhang, J., Zhang, H., and Li, L. (2018). Neoproterozoic tectonic transition in the South Qinling Belt: new constraints from geochemistry and zircon U–Pb–Hf isotopes of diorites from the Douling Complex. *Precambrian Res.* 306, 112–128. doi:10.1016/j.precamres.2017.12.043
- Zhang, Q., Zhang, Z. Q., Sun, Y., and Han, S. (1995b). Trace element and isotopic geochemistry of metabasalts from Danfeng Group (DFG) in Shangxian Danfeng area, Shaanxi province. *Acta Petrol. Sin.* 11, 43–54.
- Zhang, R. Y., Sun, Y., Zhang, X., Ao, W. H., and Santosh, M. (2016). Neoproterozoic magmatic events in the South Qinling Belt, China: implications for amalgamation and breakup of the Rodinia supercontinent. *Gondwana Res.* 30, 6–23. doi:10.1016/j.gr.2015.06.015
- Zhang, S. G., Wan, Y. S., and Liu, G. H. (1991). *Metamorphic Geology in kuangping group, North Qinling*. Beijing: Science and Technology Press, 1–119.
- Zhao, J. H., and Zhou, M. F. (2009). Secular evolution of the Neoproterozoic lithospheric mantle underneath the northern margin of the Yangtze Block, South China. *Lithos* 107, 152–168. doi:10.1016/j.lithos.2008.09.017
- Zhao, L. M., Li, Y. L., Xiang, H., Wang, G. Q., Zheng, J. P., Xiao, W. J., et al. (2021). Meso-Neoproterozoic arc-related sediments of the Xiahe Group in the Qinling block, Central China: implications for the paleogeographic reconstruction of Rodinia. *Precambrian Res.* 361, 106263. doi:10.1016/j.precamres.2021.106263